A GIS-BASED TEMPERATURE MODEL FOR THE PREDICTION OF MAXIMUM STREAM TEMPERATURES IN THE CASCADE MOUNTAIN REGION

Amy L. Sansone
Dennis P. Lettenmaier

Department of Civil Engineering
University of Washington
Seattle, Washington 98195

A GIS-BASED TEMPERATURE MODEL FOR
THE PREDICTION OF MAXIMUM STREAM TEMPERATURES
IN THE CASCADE MOUNTAIN REGION

by

Amy L. Sansone
Dennis P. Lettenmaier

December 2001

ABSTRACT

Water quality changes associated with timber harvesting have long been a concern of environmental planners and regulators. Removal of streamside vegetation clearly changes the energy balance of a stream, and hence its temperature. A common approach to mitigating such effects is to require that buffer zones be established along stream corridors, within which vegetation is not to be disturbed by logging. To evaluate the performance of such measures, we describe a simple energy balance model, STRTEMP, for prediction of stream temperature in forested watersheds. The model has two structural components. The first estimates shortwave radiation incident to the stream surface, accounting for shading due both to topographic features and the effects of streamside vegetation. The second component uses the predicted stream surface downward solar and longwave radiation along with other meteorological and physical parameters to solve the stream reach energy balance for stream temperature. The model is intended for estimation of "worst case" or maximum annual temperature, and is therefore applied on an event basis to low flow conditions, and maximum annual solar radiation and air temperature. Low flow conditions were defined as the 7-day 10-year low flow (7Q10), which was estimated by a regional regression equation in which catchment characteristics readily accessible from GIS data bases (e.g., precipitation, and topographic characteristics) were the independent variables, and estimated 7Q10 values at USGS gaging stations were the dependent variables. These equations were then applied to estimate the reference 7Q10 values over a domain that included the forested portions of the Washington Cascades. Reference annual temperature values were obtained from a national data set produced for climatalogical studies by the University of Washington. The model was calibrated using field data collected in the Beckler and Entiat River basins on the west and east slopes of the Cascades, respectively. Model performance was then evaluated through comparison of predicted maximum reach temperatures with independent USFS observations for 10 stream reaches within the Suiattle and Twisp River basins on the west and east slopes of the Cascades, respectively. Insofar as the observations were not continuous, the model was expected to predict maxima that exceeded the maximum of the observations, which was the case for all except one site in the Twisp River drainage. A series of sensitivity analyses were conducted for various physical characteristics of stream buffers. The results showed that in general, increasing the buffer width beyond 30 meters did not significantly decrease stream temperatures. Other vegetation parameters such as average tree height, and to a lesser extent stream width, average canopy height and leaf area index (LAI) appeared to have a stronger effect on maximum stream temperatures.

ACKNOWLEDGMENTS

TABLE OF CONTENTS

LIST OF FIGURES

LIST OF TABLES

viii

CHAPTER 1: INTRODUCTION

1.1 OVERVIEW

Water quality changes associated with timber harvesting have been a concern of environmental planners and regulators at least since the 1960's (Salo and Cundy, 1987). In particular, logging of near stream vegetation affects water quality by changing the physical inputs into and the energy balance of a stream. Riparian vegetation stabilizes the banks, intercepts some of the precipitation and blocks and diffuses incoming radiation from the sun (Selby, 1993, Chapter 12; Monteith and Unsworth, 1990, Chapter 6). Riparian vegetation also provides large woody debris (LWD) and allocthonous inputs to the stream. Figure 1.1 below shows an example of clearcutting along a stream.

Figure 1.1: Photograph of clearcutting on Rockpile Creek in Northern California. Taken by the Gualala River Improvement Network.

As evidenced by the photograph, removal of the streamside vegetation, eliminates a source for LWD, exposes the soil to increased erosion and modifies the energy balance of the stream.

The energy balance of a stream is determined by the incoming radiation from the sun, the radiation emitted from the earth's surface, water-air interactions, stream-streambed interactions and incoming groundwater and streamflow. Riparian vegetation plays an important role in the energy balance in headwater streams. The most important of these influences is buffering the stream from incoming solar radiation.

Elevated stream temperatures affect all aspects of the aquatic environment including the type and abundance of primary producers, the life stage cycles of benthic invertebrates and fishes and the chemical composition of the water (Hynes, 1970). In headwater streams where dense forest cover limits the heating of the stream during the day and minimizes diurnal fluctuations fishes have become adapted to specific temperature ranges. When headwater streams are logged, the temperature changes can be devastating to aquatic life.

The Washington State Joint Natural Resources Cabinet (WSJNRC, September 1999) found that elevated temperatures were the second major cause (after bacteria) of Washington streams not meeting Water Quality Standards under the federal Clean Water Act of 1972 and that water temperature, the level of dissolved oxygen and acidity were critical factors for salmon spawning and rearing. Forests cover almost half of the State of Washington and most of the salmon-bearing streams have their headwaters in forested regions (WSJNRC, September 1999). Figure 1.2 shows the spatial extent of forests in Washington State.
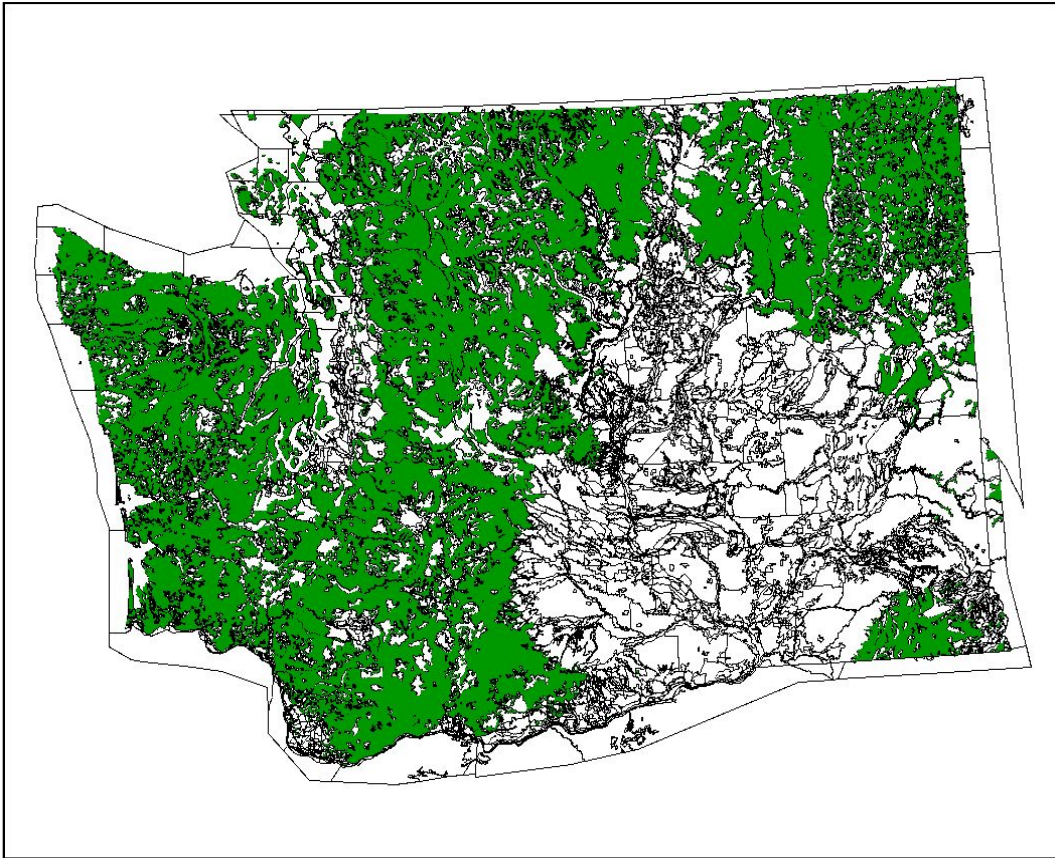
Figure 1.2: Extent of Forest Cover in Washington State. Courtesy of the National Gap Analysis Program of the Biological Resources Division of the USGS (USGS, 1995).

19 Washington salmon, steelhead and trout fish populations have been listed under the Endangered Species Act (ESA) as threatened or endangered since 1992. A critical aspect of the development of recovery plans under ESA is the requirement for accurate prediction of stream temperature changes due to logging. 67% of the forest lands in the State are now covered with young trees due to logging over the past 30 years. In general, this change in vegetation maturity has reduced the quality of fish habitat (WSJNRC, September 1999).

Land cover changes due to logging, combined with the conversion of forests to urban land, especially in lowland regions, makes protecting salmonid bearing streams in headwater regions particularly important. Washington State supports chinook, chum, pink, sockeye, and coho salmon, as well as steelhead, bull trout and coastal cutthroat trout. Bull trout in particular can be found in almost every region of the state and have been listed as threatened in the Columbia River, Puget Sound and Washington Coastal regions. Figure 1.3 shows the regions of Washington State and the species listed under the ESA.

- Chinook listed as "threatened" 3/24/99
- Hood Canal Summer Chum listed as "threatened" 3/25/99
- Bull Trout listed as "threatened" 11/1/99

- Spring-run Chinook listed as "endangered" 3/24/99
- Steelhead listed as "endangered" 8/18/97
- Bull Trout listed as "threatened" 6/10/98
- Westslope Cutthroat Trout potential for "threatened"

- Bull Trout listed as "threatened" 6/10/98
- Westslope Cutthroat Trout high potential for "threatened"

Northeast Washington Population = 113,500

Puget Sound Population = 3,788,700

Upper Columbia River Population = 115,200

Washington Coastal Population = 179,700

Middle Columbia River Population = 395,000

Lower Columbia River Population = 464,000

Snake River Population = 82,900

- Lake Ozette Sockeye listed as "threatened" 3/25/99
- Bull Trout listed as "threatened" 11/1/99
- Southwest Washington Coho designated as "candidate" for ESA listing 7/14/97
- Coastal Cutthroat Trout proposed as "threatened" 6/5/99

- Chinook listed as "threatened" 3/24/99
- Chum listed as "threatened" 3/25/99
- Steelhead listed as "threatened" 3/19/98
- Bull Trout listed as "threatened" 6/10/98
- Coastal Cutthroat Trout proposed as "threatened" 6/5/99
- Coho designated as "candidate" for ESA listing 7/14/97

- Steelhead listed as "threatened" 3/25/99
- Bull Trout listed as "threatened" 6/10/98
- Westslope Cutthroat Trout high potential for "threatened"

- Steelhead listed as "threatened" 8/18/97
- Sockeye listed as "endangered" 11/20/91
- Spring/Summer-run Chinook listed as "threatened" 4/22/92
- Fall-run Chinook listed as "threatened" 4/22/92
- Bull Trout listed as "threatened" 6/10/98

Figure 1.3: Endangered Species Act Listings of Salmon, Trout and Steelhead. Courtesy of the Washington State Governor's Salmon Recovery Web Page (September, 2000)

To address the issue of changed (generally elevated) stream temperatures following logging, "best management practices" (BMP's) have been implemented in states with silviculture activities under the Clean Water Act. In Washington State, buffer zone widths are established under the Forest Practices Rules (WAC 222-30-040) for both Eastern and Western Washington and vary depending on the classification of the stream, classification of the adjacent land, the management harvest technique and the stream size.

The BMP most often implemented is to leave a fixed width "buffer zone" along the stream within which the vegetation is not disturbed by logging (Rishell et al., 1982; Brosofske et al., 1997). Computer models of varying complexity have been developed to help managers and planners predict the effects of buffers on stream temperatures. In the State of Washington, due to the listing of native salmon species as "endangered" or "threatened" under the Endangered Species Act, accurate prediction of summer stream temperatures in fish bearing streams has become an important issue for forestry and fisheries managers.

In forested, headwater streams, such as those found on the east and west slopes of the Cascade Mountains in Washington State, streambank vegetation serves three important purposes. It provides a food source in the form of allocthonous inputs (needles, leaves and twigs), habitat and shelter in the form of large woody debris and it helps regulate stream temperatures. Removal of riparian vegetation can result in increases in the magnitude of diurnal temperature fluctuations, increases in the maximum water temperature and decreases in the minimum temperature in a stream. The magnitude of these changes is dependent upon the amount of vegetation removed, stream width, depth and discharge, stream orientation and the amount of solar radiation reaching the stream (Lynch et al., 1977).

Elevated water temperatures have both direct and indirect effects on aquatic communities. Dissolved oxygen (DO) levels decrease and primary production increases with increasing stream temperature (Chapra, 1997). Fish mortality occurs if DO drops below species-dependent critical levels. Increased temperatures also cause more fine material to settle (Hynes, 1970). Settling of fine material can have deleterious effects for invertebrate and fish species that use the interstitial spaces between the substrate as habitat. The prevalence of different types of benthic fauna and the time of emergence varies with stream temperature as well (Hynes, 1970; Lee and Samual, 1976). This effects the quality and type of food available to invertebrate and fish species downstream.

Temperature also affects the spawning time, growth rate, incubation, migration and emergence times for fishes. Higher temperatures may also cause species seeking lower temperatures to migrate upstream, displacing other species normally found in that particular habitat (Lynch et al., 1984; Lynch et al., 1977). Although the temperature may recover relatively quickly downstream of logged headwater streams the effects of increased temperatures on the chemical composition of the water and on the type and amount of biomass traveling downstream may be more persistent.

Solar radiation is the most important factor determining temperature change in streams affected by logging (Brown, 1969). Temperature patterns in headwater streams are particularly affected by changes in stream incident solar radiation resulting from shade removal due to their small volume (Brown and Krygier, 1970). In general, the effects of shading on stream temperature decreases with increasing stream size. Buffer widths can mitigate the effects of logging on stream temperature in small streams by maintaining shade over the stream (Lee and Samual, 1976). Diurnal fluctuations and maximum and minimum temperatures change significantly from pre-logging levels when riparian vegetation is removed and can reach levels detrimental to fishes. Depending on the width, buffer zones that maintain stream shading have a mitigating effect on these changes (Lynch et al., 1984). Brosofske et al. 1997 found for some small streams in the foothills of the western Cascades that gradients in microclimate existed from the stream to the uplands and were affected by harvesting. Retention of stream buffers helped maintained these gradients. (Brosofske et al., 1997). Although the benefits of maintaining riparian buffers have been established, there is less agreement on what constitutes a sufficient buffer width. Furthermore, buffer width requirements for small, non fish-bearing headwater streams have not been established (Brosofske et al., 1997).

Computer models can be an effective tool for predicting stream temperatures and evaluating the effectiveness of BMPs. Initially, water temperature models were developed to predict temperature changes in large rivers and lakes due to dams and

heated effluent discharges (Brown, 1969; Sartoris, 1976; Jaske, 1965). These applications contrast with those of interest to forest managers, which are usually small streams in forested mountainous regions. To predict stream temperatures accurately in such environments, models are needed that take into account both topographic and vegetation effects on the energy balance. Different components of the energy balance are important when modeling small streams as opposed to large rivers. Groundwater advection and conduction between the stream and the streambed are often insignificant when modeling large rivers but may be significant for small streams (Brown, 1969). When modeling small streams, complete lateral and depth mixing (one-dimensional assumption) may be appropriate whereas in large rivers vertical temperature gradients are often significant (Hynes, 1970).

Various physically based models have been developed for modeling temperature in small mountain streams (Theurer, 1984; Sullivan et al., 1990). Although these models evaluate the effects of shading on stream temperature, they are often complex and require data that are not readily available. Planners and managers may not have the resources or the technical expertise to invest in these models.

The Timber/Fish/Wildlife Temperature Workgroup in Washington State (TFW) evaluated a group of computer models which they felt would be applicable to forest management planning (Sullivan et al., 1990). The TFW evaluated the models to determine the best one for characterizing in a simple and efficient way streams which may be particularly sensitive to temperature increases caused by forest harvesting. They concluded that an empirical relationship was the best for use by forest managers. The empirical relationship, known as the Temperature Sensitivity Screen (TFW 1990) does not predict a specific temperature but places a site in a category based on water quality standards.

The TFW relationship does not account for critical factors that affect stream temperature such as variations in streamflow, geometry of vegetation cover, cumulative effects of upstream disturbances, and stream orientation (LaMarche et al., 1997). La Marche et al. (1997) developed a simple model based on the energy balance to incorporate some of these critical factors not addressed by the TFW's empirical relationship. This thesis generalizes the LaMarche et al method to be applicable to any forested landscape, and examples are developed for the east and west slopes of the Cascade Mountains, Washington.

1.2 OBJECTIVES

The purpose of this research is to develop a GIS-based stream temperature model which, while based on physical principals, is easily implemented, and accurately predicts maximum stream temperatures during the critical summer low flow period. The model incorporates the STRTEMP energy balance model (LaMarche et al., 1997) and is designed to replace empircial approaches like the Sullivan et al. (1990) algorithm currently incorporated in the Washington Forest Practices Manual. The intent of the model developed here is twofold. The first intent is to provide the basis for determining a potential maximum stream temperature based on 7 day 10 year low flow (7Q10 flow) and 10 year maximum air temperature in forested mountain streams. The second intent is to provide a basis for determining the effects of differing vegetation parameters on the potential maximum stream temperature. The model is simple enough to use to be applicable in forest management and planning.

1.3 APPROACH

The approach used here is based on the STRTEMP model of LaMarche et al. (1997). The stream temperature model is linked with a digital elevation model in GIS (ARCINFO) format. The model has three components: a GIS component which allows

the user to choose the stream of interest, a shortwave radiation component which takes into account shading due to topography and streamside vegetation and a one-dimensional stream energy balance component which predicts stream temperature along a reach. The model is menu driven in ARCINFO and has the capability of using model-derived default values for stream characteristics and meteorological data or can use data provided by the user.

CHAPTER 2: BACKGROUND

2.1   Stream Temperature Processes

2.1.1 Heat Balance

Contaminant tranport modeling is based on a mass balance which equates the change of mass in a control volume to the sum of the net flux through the volume plus sources and sinks. This is known as the advective-diffusion equation and describes the flux of a contaminant through a system. An advective-diffusion equation can also be written for heat. The change in heat in a control volume is the sum of the net heat flux through the volume plus sources less sinks (Chapra, 1997). The net heat flux has two components; advection and diffusion. Advection is the transport of heat due to the motion of the fluid and diffusion is the transport of heat in the direction of decreasing temperature (Handbook of Hydrology,Chapter 14,1993).

The general form of the advective-diffusion equation is

$$\frac{\partial T}{\partial t} = -U\frac{\partial T}{\partial t} - V\frac{\partial T}{\partial t} - W\frac{\partial T}{\partial t} + D_x\frac{\partial^2 T}{\partial x^2} + D_y\frac{\partial^2 T}{\partial y^2} + D_z\frac{\partial^2 T}{\partial z^2} + \frac{S}{\rho c_p d}$$

where,

U , V , and W are velocity components in the x, y and z directions

T is the temperature

D_x , D_y , and D_z are the turbulent diffusivities in the x, y and z directions

S is the net heat exchange

ρ is the density of water

c_p is the specific heat of water

d is the depth

It is assumed that turbulent diffusion is the dominant diffusive process and therefore molecular diffusion, which is several orders of magnitudes smaller, can be ignored. When the 3-D advective-diffusion equation is simplified to 1-D or 2-D the differential advection caused by the variation of velocity from zero at the stream boundaries to a maximum is no longer accounted for. This differential advection skews the spatial average temperature and is accounted for in the 1-D and 2-D simplifications through a shear-flow, or longitudinal, dispersion coefficient.

For natural streams, when investigating temperature changes from upstream to downstream, a one dimensional analysis is often used. The general form of the advective-diffusion equation becomes a 1-D equation with the following simplifications.

- The velocity in the transverse and vertical directions are averaged to zero causing those two velocity terms to drop out.
- The system is assumed well mixed so that the change in temperature in the transverse and vertical directions is zero causing those two diffusivity terms to drop out.
- The longitudinal dispersion is 2 to 3 orders of magnitude larger than the turbulent diffusivity in the longitudinal direction so the turbulent diffusivity is ignored.

The 1-D equation, also called the advective-dispersion equation (Sinokrat and Stefan, 1993), for heat flux in the longitudinal direction assuming a well mixed flow system is

$$A\frac{\partial T}{\partial t} + \frac{\partial(QT)}{\partial_x} = \frac{\partial}{\partial_x}\left(AD_L\frac{\partial T}{\partial x}\right) + \frac{wS}{\rho c_p}$$

where,

Q is streamflow

T is temperature

D_L is the longitudinal dispersion coefficient

S is the net heat exchange

ρ is the density of water

c_p is the specific heat of water

A is the cross sectional area

w is the wetted width of the cross section

t is time

x is distance in the longitudinal direction

For a constant cross section and flow, the equation reduces to

$$\frac{\partial T}{\partial t} = -U\frac{\partial T}{\partial x} + D_z\frac{\partial^2 T}{\partial x^2} + \frac{S}{\rho c_p d}$$

where all terms are the same as defined in the above two equations. In the case of stream temperature, the net heat exchange, S, is a function of advection, diffusion and dispersion of heat from upstream, tributary and groundwater inflows, streambed heat flux and water-atmosphere heat exchange. (Sinokrat and Stefan, 1993).

2.1.2   Net Heat Exchange

The heat transfer between the stream and its surrounding environment is composed of the net heat exchange between the water and the atmosphere and the net heat exchange between the water and the streambed. The heat exchange between the air and the stream is governed by four main processes; heat input from solar radiation, heat loss/gain from

longwave radiation, heat loss due to evaporation (latent heat) and convection of heat across the air-water interface (sensible heat). The heat exhange between the streambed and the stream is governed by heat loss/gain from conduction.

Solar radiation provides the energy that drives physical and biological processes at the earth's surface during the day and is the component in the energy balance most affected by changes in streamside vegetation. Scattering and absorption in the atmosphere attenuate the solar radiation that reaches the earth's surface. Scattering changes the direction of radiation and is caused by the interactions between radiation and molecules of gas in the atmosphere and between radiation and aerosals (e.g., particles of dust, pollen, smoke, and water vapor) in the atmosphere. Absorption by ozone, carbon dioxide and water vapor attenuates the radiation that reaches the surface, resulting in heating of the atmosphere. The total radiation that reaches the earth's surface is the sum of direct radiation, coming from the direction of the sun, and diffuse radiation, coming from all other scattered radiation. The change in total radiation throughout the day is approximately sinusoidal for both clear sky and cloud cover and varies both daily and seasonally (Monteith and Unsworth, 1990).

The longwave radiation is the net of black body radiation emitted by the atmosphere incident on the surface and black body radition emitted by the earth's surface. On average, the surface of the earth is warmer than the atmosphere resulting in a net loss of energy from the surface. Over a day the net longwave radiation remains relatively constant compared to the shortwave radiation which peaks at solar noon. The downward flux of longwave radiation from the atmosphere is higher under cloudy conditions and the upward flux from the surface tends to be higher in the summer.

Evaporation is a diffusive process which results in the loss of heat from the evaporative surface. The evaporation rate is dependent upon the vapor pressure gradient between the air and water surface, wind, temperature, atmospheric pressure and net radiation.

Convection is the transfer of heat by moving air which results in a loss of sensible heat. Sensible heat is a function of the temperature gradient at the surface, wind, and an exchange coefficient. Evaporation and convection can be related through the Bowen ratio (Bowen, 1926).

Heat conduction between the water and the streambed can be an important component of the energy balance, particularly for small streams with rocky bottoms (Brown, 1969). Conductance is the transfer of heat due to molecular interactions and for the case of streambed-stream interactions is dependent on the thermal conductivity of the streambed and the streambed temperature. (Sinokrat and Stefan, 1993).

2.2   Stream Temperature Models

Most computer models used to predict stream temperature in forested, mountain regions are one-dimensional, and assume a well mixed system. These two assumptions are appropriate because due to the small size of mountain streams the main variation in temperature is in the flow and one can assume the system is well mixed. On a daily average basis, solar radiation is usually the largest term in the energy balance for small streams (Brown, 1969). To predict the incident solar radiation term in the energy balance of mountain streams accurately, the topographic and vegetative shading must be represented.

Stream temperature models can be grouped in one of two categories; reach models and basin models. Reach models were developed to evaluate water temperatures in a reach of a stream with similar physical characteristics and do not take into account groundwater and tributary inflows. Basin models evaluate entire watersheds by calculating the temperature of individual reaches and then routing the heat downstream. Basin models evaluate the heat exchange from groundwater and tributary inflows. The GIS-STRTEMP model developed here is a reach model. Some of the more common reach models are

Brown's Equation, TEMP-86 and SSTEMP (Sullivan et al., 1990). Brown's Equation calculates water temperature at a point and has been widely used in forestry. It has the following form.

$$T_w = (\Delta SA / F)0.000267$$

where,

T_w is water temperature ($°F$)

ΔS is the net change in energy stored (Btu / ft^2 min)

A is the surface area of the study reach (ft^2)

F is the discharge (cfs)

The net change in energy stored, ΔS, is a function of the net thermal radiation flux measured in the field and the evaporative, conductive, convective and advective fluxes. Brown's equation assumes the net radiation measured in the field is an accurate representation of the radiation flux over the stream during a day. The equation also assumes that advective inflow and groundwater inflow are negligible (Brown, 1969). Some other reach models in wide use are the SSTEMP model (Theurer et al., 1984) and the TEMP-86 model (Beschta, 1984). The SSTEMP model assumes a one-dimensional well-mixed system and consists of both a heat flux and a heat transport model to calculate the longitudinal change in water temperature over time. The heat flux component contains a solar radiation model which takes into account shading due to topography and riparian vegetation. The TEMP-86 model is similar to the SSTEMP model with a more detailed analysis of shading effects (Sullivan et al. 1990). A more detailed description of the SSTEMP and TEMP-86 models can be found in Theurer et al., 1984 and Beschta 1984, respectively.

2.3   The TFW Temperature Screen

The Washington Timber, Fish, and Wildlife Temperature Workgroup performed a detailed review of several of the stream temperature prediction models currently in use (TFW, 1990). TFW evaluated the SSTEMP, TEMP-86 and TEMPEST reach temperature models and the QUAL2E, USFWS-SNTEMP and MODEL-Y basin temperature models in the context of a larger study which evaluated stream temperature regimes in Washington State. Among the objectives of the study were to evaluate and select a method of temperature prediction for use by forest regulators, to establish general stream temperature regimes for ecoregions in Washington State, and to evaluate temperature sensitivity screening criteria. Water temperature, air temperature and stream and riparian characterisitics were measured at 33 primary sites and water temperature was measured at 59 secondary sites throughout the state. Water temperature was only measured at the downstream end of the temperature reaches. Many of the sites were clustered in the Southwest Cascades region. The data were collected in the summer of 1988 and were used to determine how well the models predicted water temperature.

Regional linear regression relationships were also developed to relate flow characteristics to watershed area and distance from watershed divide for use in some of the models. Most of the relationships were based on data collected at the 33 primary sites. For instance. relationships between flow and basin area were developed. Where a stream gage existed in a basin, the August mean unit flow rate was determined and multiplied by basin area to obtain streamflow. In ungaged basins a regression relationship was used to obtain streamflow. To estimate stream velocity a relationship between stream velocity and distance from watershed divide was developed, except where the distance was less than 3 km in which case 0.05 m/s was assumed. Groundwater inflow rate was assumed to equal the average streamflow divided by the distance from watershed divide. Groundwater temperature was assumed to equal the mean annual air temperature

obtained from an temperature isotherm map for the state of Washington. Regression relationships were developed for stream width and depth, although field measurements were used in the model analyses. Regression relationships were also developed for the sky view factor in mature forest streams.

A sensitivity analysis of the predicted water temperature to selected input parameters was performed. The parameters tested were limited to those that could be measured, and to values within the range expected in Washington streams. Default values for the input parameters in question were determined from field and weather station data. All parameters were assigned the defaults except one which was varied over the range of possible values. The results showed that wind, groundwater, dust reflectivity and ground transfer coefficients showed little sensitivity whereas air temperature and relative humidity showed high sensitivity.

After evaluating the temperature models based on accuracy and ease of use TFW concluded that all of the models evaluated were either too complex and required data not readily available or did not predict stream temperatures accurately. An empirical relationship was developed based on the 1988 data. Based on elevation and percent shade, stream temperatures fall in either a low, moderate or high category. The categories were determined based on existing state and federal regulations for stream temperature thresholds. The empirical relationship, known as the Temperature Sensitivity Screen (TFW 1990) does not predict a specific temperature but places a site in a category based on water quality standards.

The TFW temperature screen nomograph is given in the Figure 2.1.
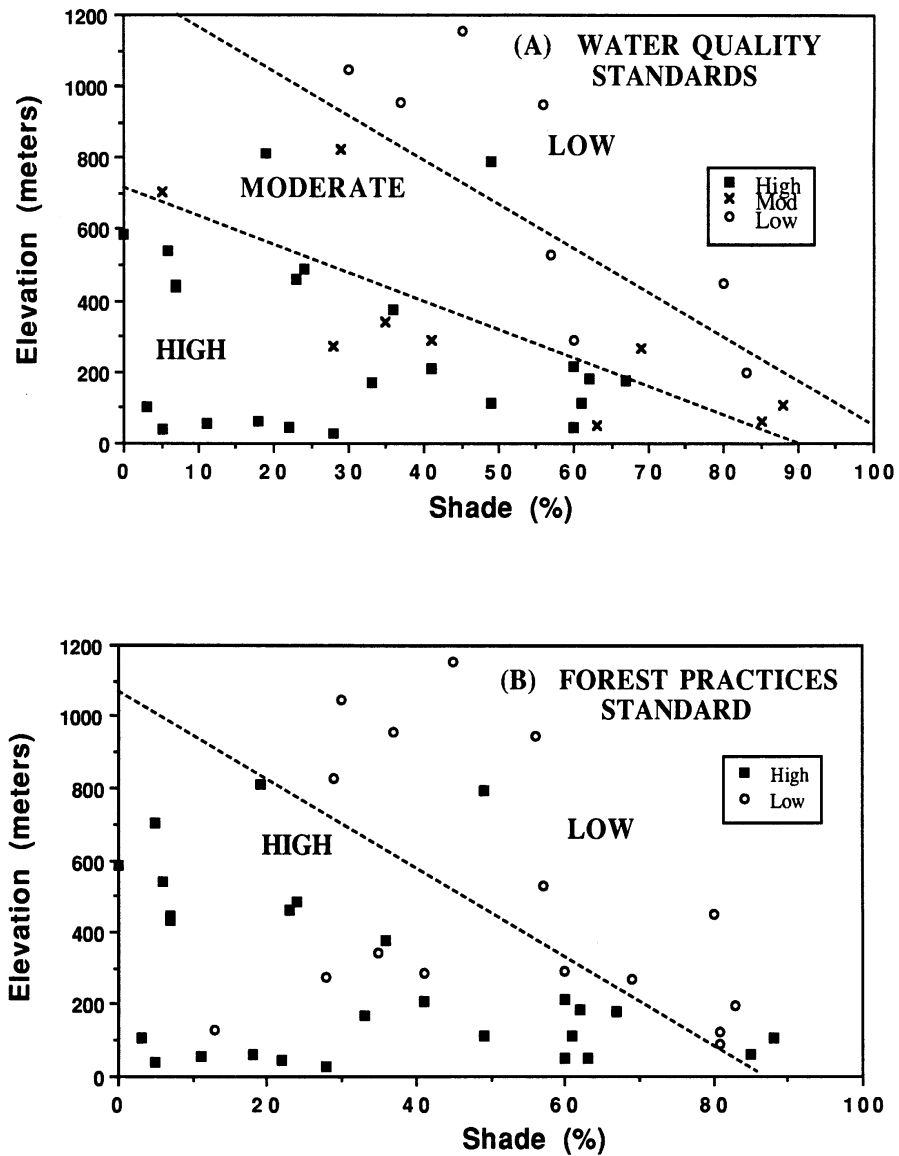
Figure 2.1: TFW Temperature Screen Monograph (Sullivan et al., 1990).

Some of the limitations of the Temperature Sensitivity Screen are as follows.

- The relationship does not predict an actual temperature but instead places the evaluation site in a category based on percent shade and elevation.

- When the relationship was tested (TFW 1990) with study site data, the results had a high amount of scatter and in some cases almost half of the data fell outside of the correct category
- Lines dividing the categories were hand drawn and not based on statistical analysis and were arbitrary.

The relationship is not based on physical processes that are important in predicting stream temperatures, particularly variations in streamflow, geometry of vegetation cover, cumulative effects of upstream disturbances, and stream orientation (LaMarche et al., 1997).

CHAPTER 3: DATA COLLECTION

3.1 BASIN DESCRIPTIONS

To evaluate the performance of the GIS-STRTEMP model Chapter 6, data were collected
for two streams, one draining the east and the other the west slopes of the Cascade
Mountains. The streams were chosen based on the following criteria:

- Unregulated flow
- Upstream catchment primarily forested

Based on these critieria, the Entiat River (Figure 3.1) was selected as the east side stream,
and the Beckler River (Figure 3.2) for the west side. Stream and air temperature
recorders were installed at sites along these two streams during the period from the end of
July to the end of September in the summer of 2000. Ancillary streamflow and canopy
architecture data were also collected at selected sites along these streams. Characteristics
of these two streams and their drainage basins are described below.

3.1.1   The Entiat River Basin

The Entiat River (Figure 3.1) drains a portion of the east slope of the Cascade Mountains
from the Cascade Crest to the the Columbia River, which it joins approximately 32
kilometers (20 miles) north of Wenatchee, WA. The headwaters lie in a glaciated cirque
on the Cascade Crest, from which the river flows southeasterly, mostly through forested
terrain, until approximately River km 32 (River Mile 20), downstream of which
vegetatation transitions to lowland shrubs. The drainage area of the Entiat basin is
approximately 907 square kilometers (350 square miles) with elevations ranging from a
maximum of 2819 meters (9249 feet) in the headwaters to 213 meters (700 feet) at the
mouth. The basin is bounded by the Chelan Mountains to the northeast and the Entiat
Mountains to the southwest.

The climate of the Entiat River basin ranges from moist alpine in the high elevations to arid shrub/steppe in the low elevations.   The mean annual precipitation ranges from 254 mm (10 inches) in the low elevations to 2300 mm (90 inches) in the moist alpine area. Approximately 75% of the annual precipitation falls between October and March. Mean summer daily air temperatures range from 15 to 21 $°C$ (60 to 70 $°F$) in the lower basin to 10 to 15 $°C$ (50 to 59 $°F$) in the higher elevations. The headwaters of the Entiat are snow-fed with winter snowfall ranging from as much as 10 meters (400 inches) on the peaks to less than one meter at lower elevations. Historically, vegetation within the Entiat basin has been affected by fires, floods, grazing and timber harvest (USDA, 1996).

STUDY AREA BOUNDARY

Lake Chelan

Cedar River

Columbia River

Mt Rainier

Mt Adams

Mt St Helens
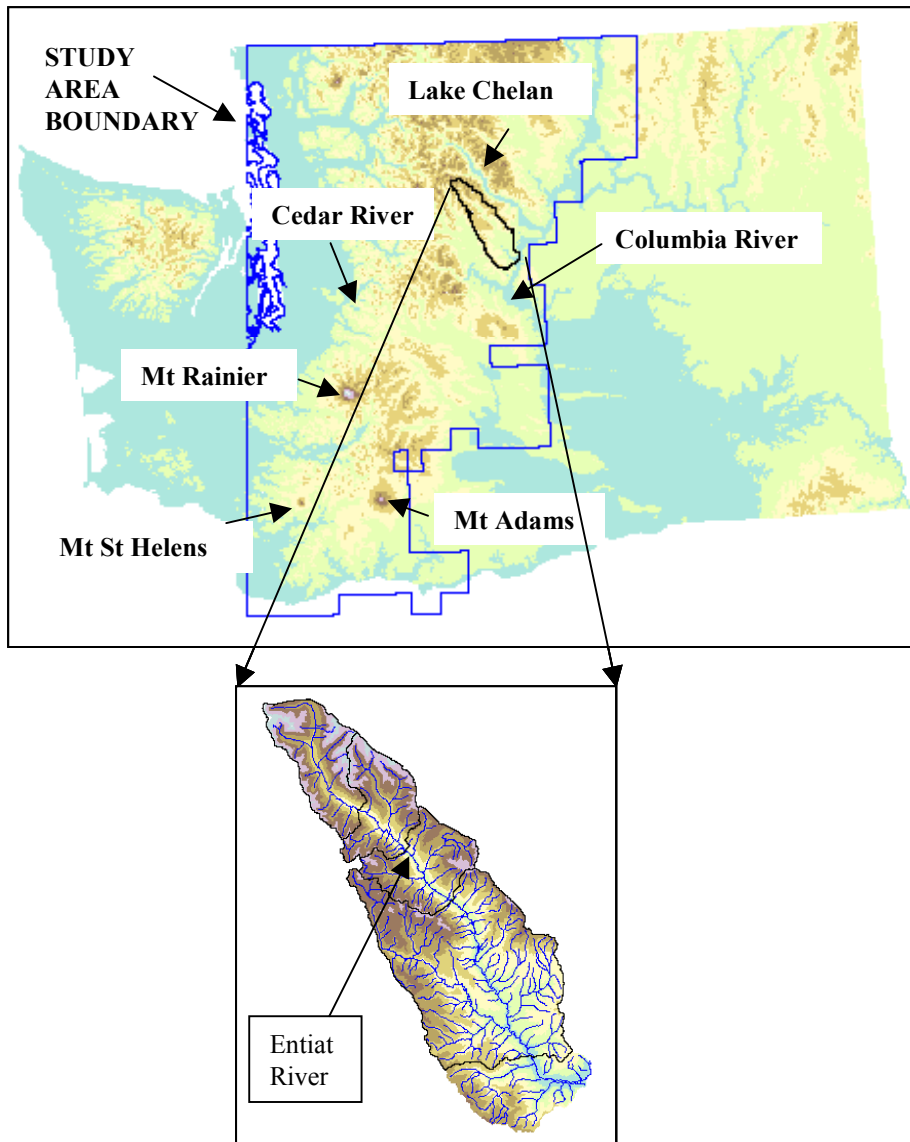
Entiat River

Figure 3.1: Location Map of the Entiat River Drainage Basin

3.1.2   The Beckler River Basin

The Beckler River (Figure 3.2) drains the west slope of the Cascade Mountains in the Mt. Baker-Snoqualmie National Forest, joining the South Fork of the Skykomish River near Skykomish, WA. The drainage area of Beckler River, from it's confluence with the

South Fork of the Skykomish River, is 260 square kilometers (100 square miles), of which its largest tributary, the Rapid River, accounts for 106 square kilometers (41 square miles). Annual average precipitation ranges from about 2700 mm (106 inches) at the mouth to 2080 mm (82 inches) in the headwaters region. An estimated 77% of the annual precipitation falls between October and March. Annual snowfall ranges from about 1.5 m (59 inches) at the mouth of Beckler River to over 12 m (472 inches) in the headwaters (Wissmar and Beer, 1994). The source of this data from Wissmar and Beer is unknown but seems to be quite high. Summer mean daily air temperatures range from 20 $°C$ (68 $°F$) in the lower basin to 10 $°C$ (50 $°F$) in the higher elevations. The main stems of both the Beckler River and the Rapid River support anadromous fish populations. Populations of coho, pink, summer chinook, chum salmon, summer steelhead, cutthroat trout and Dolly Varden have been observed in both the Beckler and Rapid Rivers. The anadromous fish are present in Beckler and Rapid Rivers due to a "trap and haul" facility on the South Fork Skykomish River where a natural barrier exists at Sunset Falls. (Wissmar and Beer, 1994).
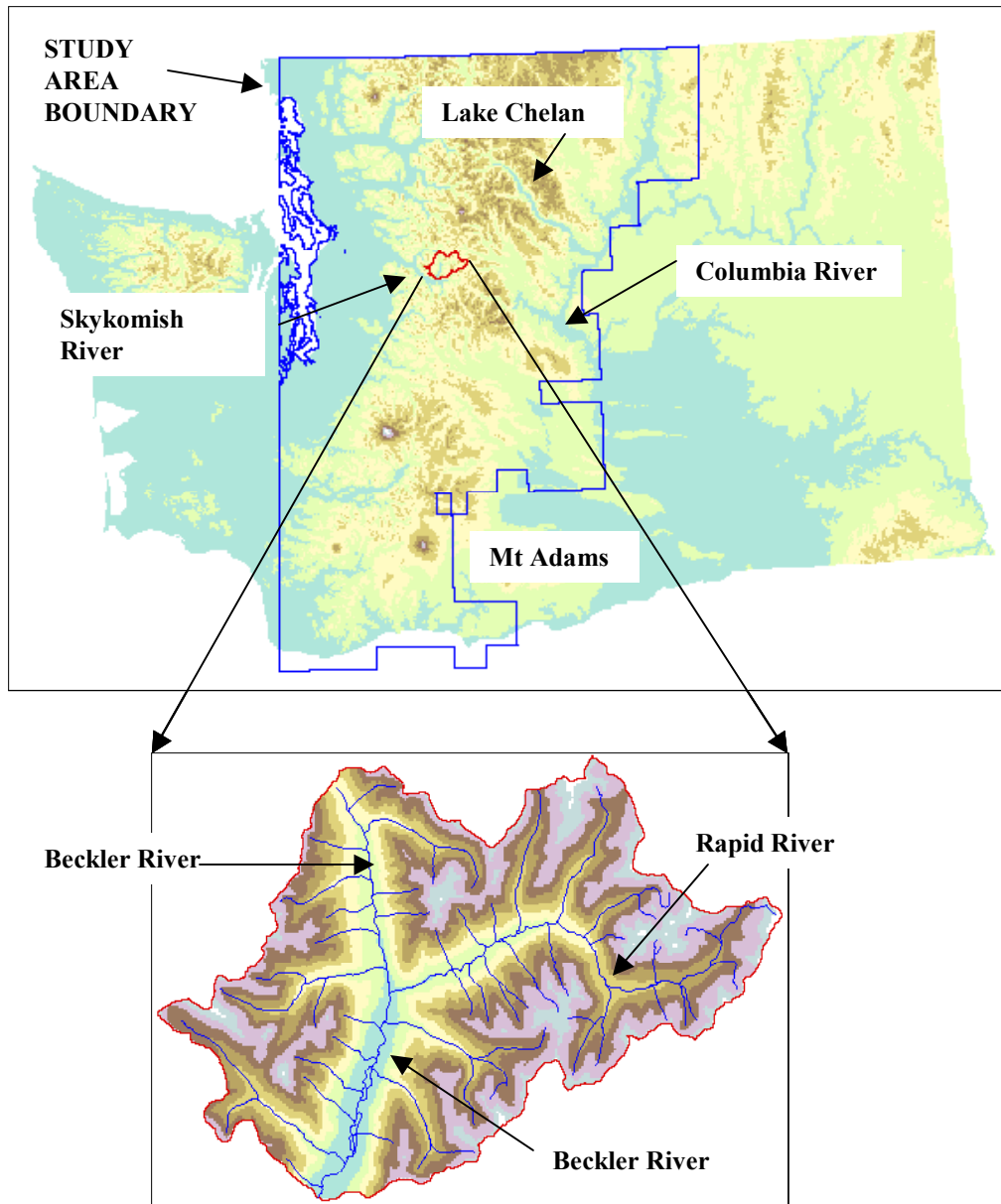
Figure 3.2: Location Map of the Beckler River Drainage Basin

3.2 EXPERIMENTAL DESIGN

Stream and air temperature data were collected at hourly intervals from the end of July to the end of September 2000 using Hobo StowAway TidBit™ data loggers from the Onset Computer Corporation. The data loggers operate in the temperature range of $-20\ °C$ to

$+50\ ^{\circ}C$ and have an accuracy of $\pm 0.4\ ^{\circ}C$. Point measurements of water temperature were also taken with a thermometer approximately weekly throughout the data collection period. The temperature loggers were placed at a minimum of three locations in each of the two streams. In addition, one logger was placed at the upstream-most and downstream-most sites in each basin to record air temperatures. The loggers were attached to the bank using plastic coated clothesline wire. Protective casings were not used. The wire was placed under rocks on the bottom of the channel to ensure it would remain in place. The wire allowed the loggers to remain suspended in the water column above the streambed. Hourly data were collected continuously from the end of July through the middle of September. The air temperature loggers were place on the banks of the stream out of direct sunlight, approximately 1.5 to 3.0 meters (5 to 10 feet) from the water's edge. Two temperature loggers were placed at each site to assure that data would be recorded even in the event of failure of one of the recorders. A description of the field sites is given in Section 3.3. The equipment located at each field site is described in Table 3.1.

Table 3.1: Description of Equipment Located at Each Field Site

Field Site	River Km	Number of Air Temperature Loggers	Number of Stream Temperature Loggers
Cottonwood	60.5 (37.6 miles)	1	2
TommyBr	49.6 (30.8 miles)	0	2
NatForestSign	40.9 (25.4 miles)	1	1
Mile6	10.0 (6.2 miles)	0	1
Rapid River	21.6 (13.4 miles)	1	2
Beckler/Rapid confluence	11.1 (6.9 miles)	0	2
Beckler Bridge	1.6 (1.0 miles)	1	2

Stream velocity and cross section were measured periodically to determine streamflow at each location where stream temperature was measured. Stream velocity was derived with

a Marsh-McBirney current meter. The current meter has a range of –0.15 to 6.09 m/sec and an accuracy of ± 0.2 % of the reading plus ± 0.015 m/sec. Cross section data were measured with a rod, level and tape measure. Canopy cover was measured with a spherical densiometer at the locations of the temperature loggers.

3.3   FIELD DATA

3.3.1 The Entiat River

Stream temperature loggers were installed at four sites along the Entiat River Road as indicated in Table 3.2.   Locations are relative to the Entiat River road intersection with US Highway 97 which has been approximated as the confluence with the Columbia River, and roughly correspond to river miles.

Table 3.2: Entiat River Site Description

Site Name	Percent Overstory Density	Description of Streamside Vegetation	Approximate Distance From Confluence with the Columbia River (km)
Cottonwood	50	Douglas Fir Predominant (w/ approx. 5% Deciduous)	60.5 (37.6 miles)
TommyBr	36	Douglas Fir Preominant (w/ approx. 10% Deciduous)	49.6 (30.8 miles)
NatForestSign	11	Ponderosa Pine/Douglas Fir Mixed (w/ approx.50% Deciduous)	40.9 (25.4 miles)

Site Name	Drainage Area (km^2)	Elevation (m)	Reach Length (m)	Streamflow (cms)	Stream Width (m)	Stream Depth (m)
Cottonwood	149	1067	4900	2.9	21.8	0.3
TommyBr	273	817	2900	4.1	21.2	0.4
NatForestSign	407	631	4900	3.2	25.9	0.5

The maximum, minimum and average stream temperatures measured with the temperature loggers for the month of August are given in Table 3.3. Forest Service stream temperature data collected in the summer of 2000 were used for comparison purposes and were provided courtesy of the USFS Entiat Ranger Station. The Entiat and Chelan Ranger Stations collected stream temperature data during the summer of 2000 with Hobo StowAway TidBit™ data loggers from the Onset Computer Corporation throughout the Entiat River basin. The Forest Service collected stream temperature data at Cottonwood Campground site near the location of the upstream temperature loggers in the GIS-STRTEMP study and the data are included for comparison purposes.

Table 3.3: Entiat River Basin Stream Temperature Measurements (August 2000)

Statistic	USFS Cottonwood (River km 60.5)	This Study			
		Cottonwood (River km 60.5)	Tommy Bridge (River km 49.6)	National Forest Boundary (River km 40.9)	Mile 6 (River km 10.0)
Maximum	12.3	12.0	13.6	16.0	20.5
Minimum	5.3	5.2	6.4	7.6	11.0
Average	8.7	8.7	10.0	11.7	15.8

The differences between the USFS values and those collected for this study at Cottonwood Guard Station are within the range of accuracy of the instrument of + or − 0.4 $°C$.

3.3.2 The Beckler River

Stream temperature data were collected at three sites along the Rapid and Beckler Rivers from July 28 through September 20, 2000. Table 3.4 Summarizes characteristics of the three sites.

Table 3.4: Rapid/Beckler River Site Locations

Site Name	Percent Overstory Density	Description of Streamside Vegetation	Approximate distance upstream from confluence with the Skykomish River (km)
Rapid River	60	Douglas Fir Predominant	21.6 (13.4 miles)
Beckler/Rapid confluence	24	Cedar/Silver Fir/Douglas Fir Mixed (60% Deciduous)	11.1 (6.9 miles)
Beckler Bridge	36	Cedar/Douglas Fir Mixed (20% deciduous)	1.6 (1.0 miles)

Site Name	Drainage Area (km^2)	Elevation (m)	Reach Length (m)	Streamflow (cms)	Stream Width (m)	Stream Depth (m)
Rapid River	38	864	2100	0.8	13.8	0.3
Beckler/Rapid confluence	175	409	1000	2.4	21.5	0.4
Beckler Bridge	253	318	1300	3.1	24.3	0.7

The maximum, minimum and average stream temperatures measured with the temperature loggers for the month of August is given in Table 3.5.

Table 3.5: Beckler River Basin Stream Temperature Measurements (August 2000)

Statistic	Rapid River (River km 21.6)	Beckler/Rapid Confluence (River km 11.1)	Beckler River Bridge (River km 1.6)
Maximum	12.7	16.0	18.0
Minimum	6.0	8.7	9.6
Average	9.4	12.3	13.5

Six temperature loggers were installed along the Rapid and Beckler Rivers to measure water temperature and two were installed to measure air temperature. Hourly data were collected continuously from the end of July through the middle of September. Point stream temperature measurements were also taken to verify the logger data.

CHAPTER 4: GIS MODEL

4.1   DIGITAL ELEVATION MODEL

The GIS temperature model described in Chapter 6 uses topographic data derived from a 10-meter Digital Elevation Model (DEM) processed by Harvey Greenburg (Department of Geological Sciences, University of Washington) which in turn is derived from USGS topographic data. The DEM covers both the east and west slopes of the Washington Cascades. The boundaries of the DEM are shown in Figure 4.1.
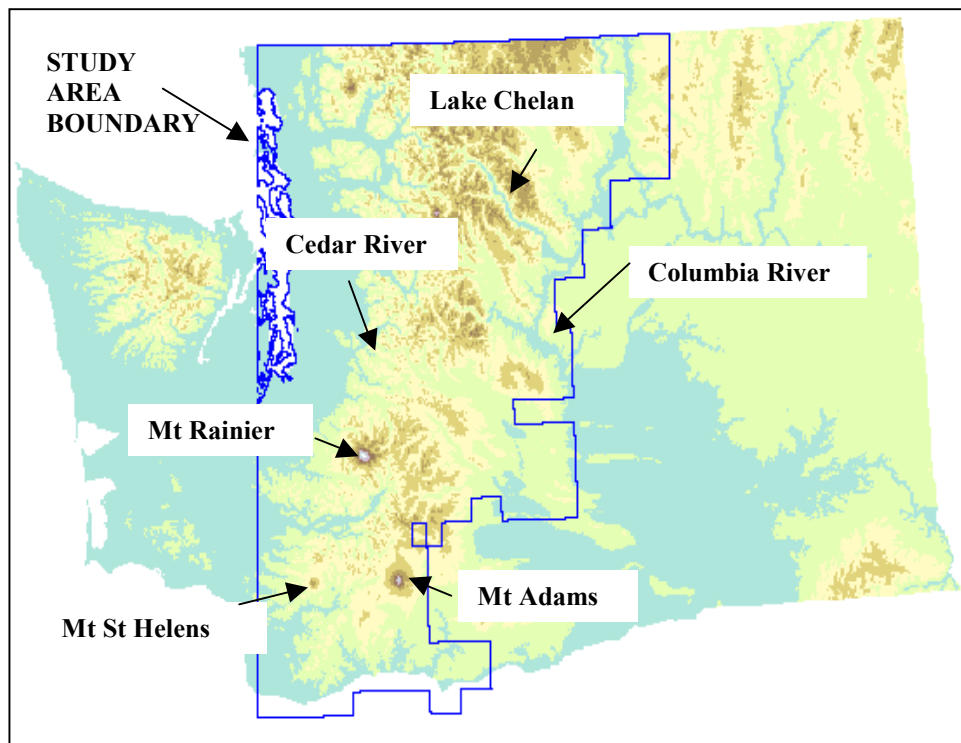
Figure 4.1: Boundary of the Cascade Mountain Region DEM.

10-meter DEM resolution was necessary to delineate the Beckler and Entiat basins and a few of the gaged basins for which USGS delineations were not available. Once the delineations were complete, the DEM was aggregated to 30 meter resolution for the 7Q10

analysis described in Chapter 5, and to 100 meter resolution for the GIS-STRTEMP model runs described in Chapter 6.

4.2   STREAM NETWORK

The stream network was obtained from the National Hydrography Dataset (NHD) developed by the United States Geological Survey (USGS) and the United States Environmental Protection Agency (USPEPA) courtesy of the USGS (http://nhd.usgs.gov/). The dataset is based on 1:100,000 resolution map data and is integrates the USGS Digital Line Graph (DLG) hydrography and the EPA Reach File Version 3 (RF3). The data are organized by reaches. The GIS model component of the GIS-STRTEMP model (Chapter 5) utilizes the NHD ARCINFO coverages to define the reach segments. Therefore, the reach lengths are predetermined, rather than being chosen by the user. The average reach length is approximately 2000 meters (1.2 miles).

4.3   WATERSHED DELINEATIONS

USGS Gage Station watershed coverages were available for most of the gaged basins within the study area that were used in the regression analysis. These data were provided by the Washington District Office of the Water Resources Division of the USGS with the understanding that they are preliminary. Basin delineations were not available for nine of the gage stations, which were therefore performed using the 10 m DEM as discussed in Section 4.1. The basin areas of both the preliminary USGS delineations and the delineations done for this analysis were checked against the areas provided by the USGS National Water Information System (NWIS) (http://water.usgs.gov/). All delineated basin areas were within three percent of the NWIS basin areas. The watershed delineations for the USGS gage stations used in the 7Q10 low flow analysis are shown in Figure 4.2.
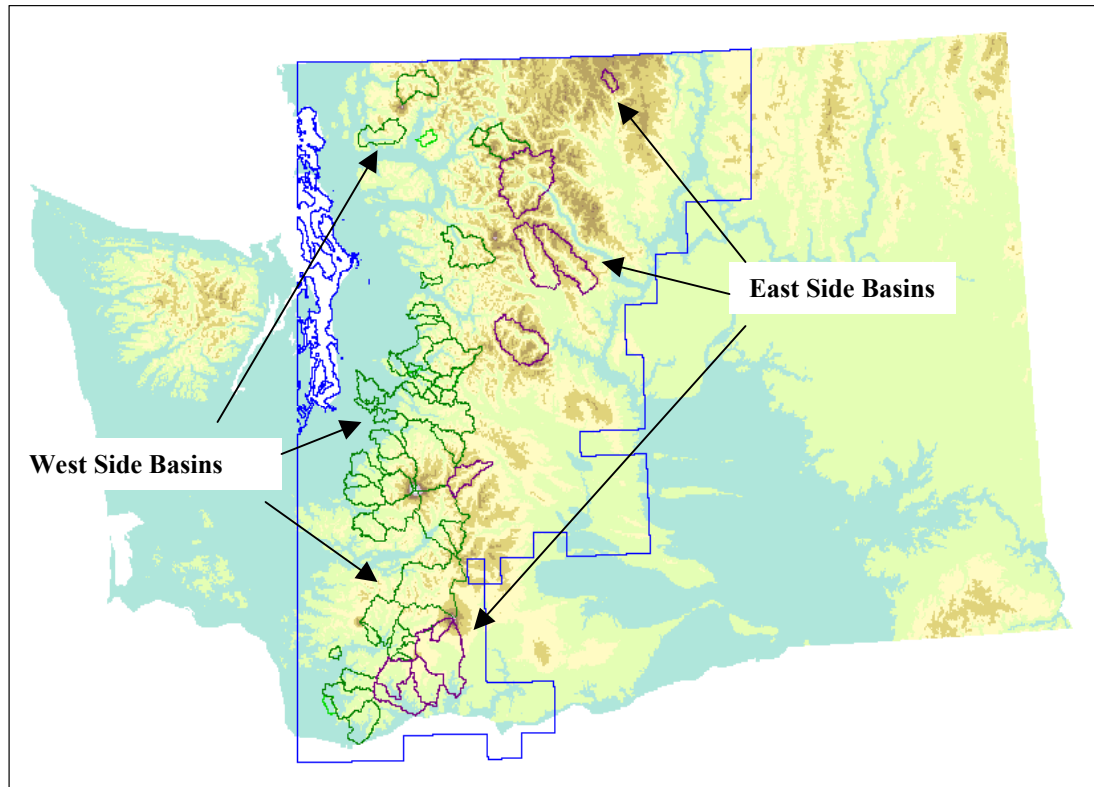
Figure 4.2: Basin Delineations for the USGS Gage Stations used in the 7Q10 low flow analysis. The dark green delineations (48 basins) are on the west side of the Cascade Mountains and the purple delineations (12 basins) are on the east side.

In addition to the Entiat and Beckler River basins used in the calibration of the GIS-STRTEMP model, the Suiattle and Twisp River basins were chosen to demonstrate use of the model. Figure 4.3 shows the location of the basins in the study area, with the Suiattle River lying on the west side of the Cascades and the Twisp River lying on the west side of the Cascades.
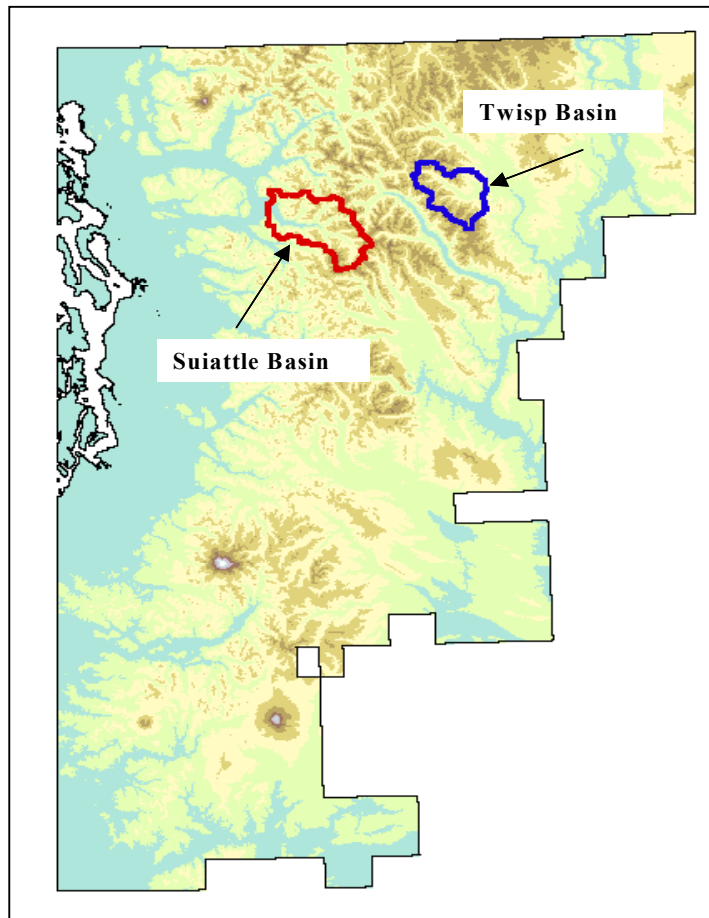
Figure 4.3: Location of the Suiattle and Twisp River Basins within the Study Area.

Simulations were performed for 10 stream reaches within each basin. The watershed delineations and the extent of anadramous fish populations for the Suiattle and Twisp River basins are shown in Figures 4.4 and 4.5, respectively.
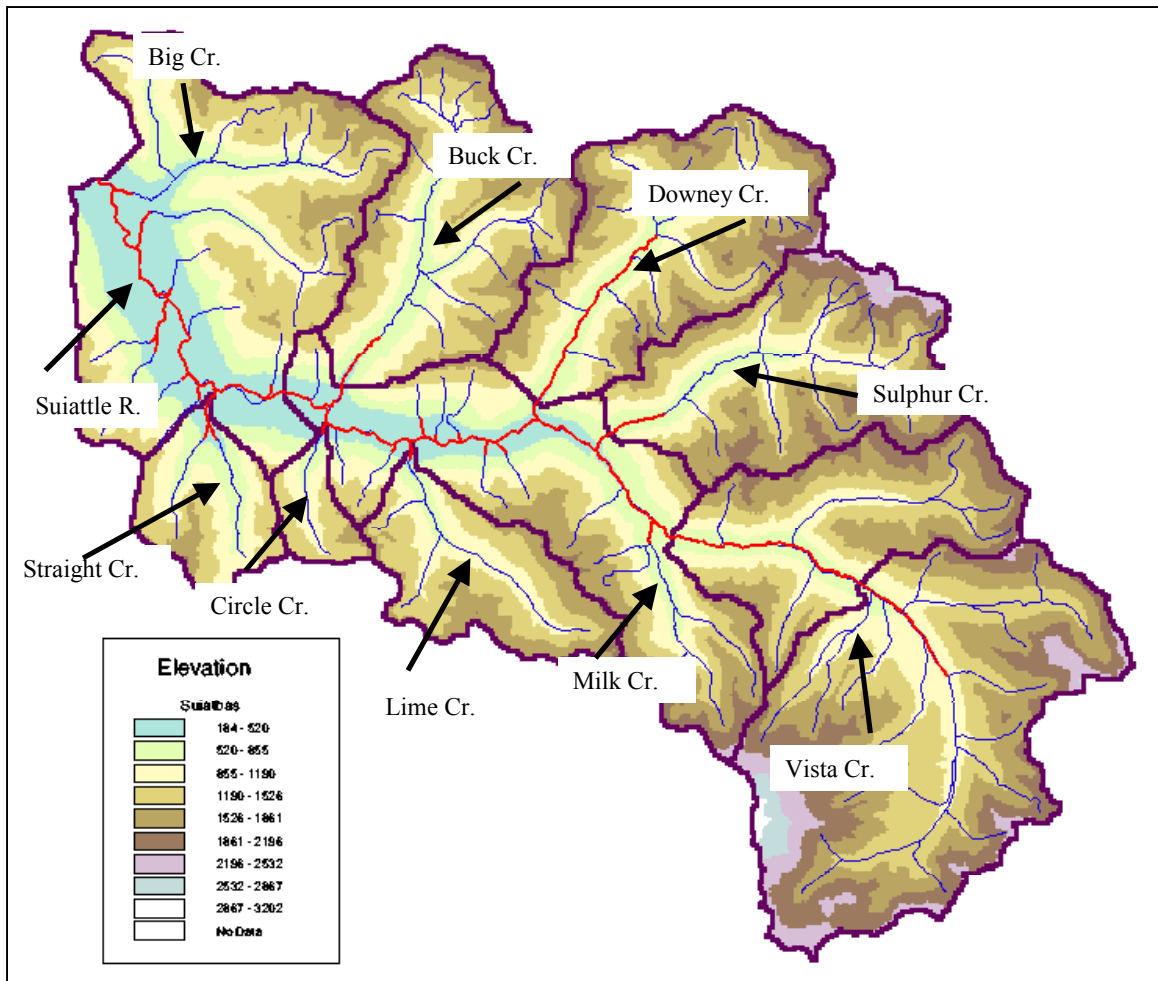
Figure 4.4: Suiattle River Subbasin Delineations. The red line indicates the extent of anadramous fish populations (courtesy of Streamnet web page).
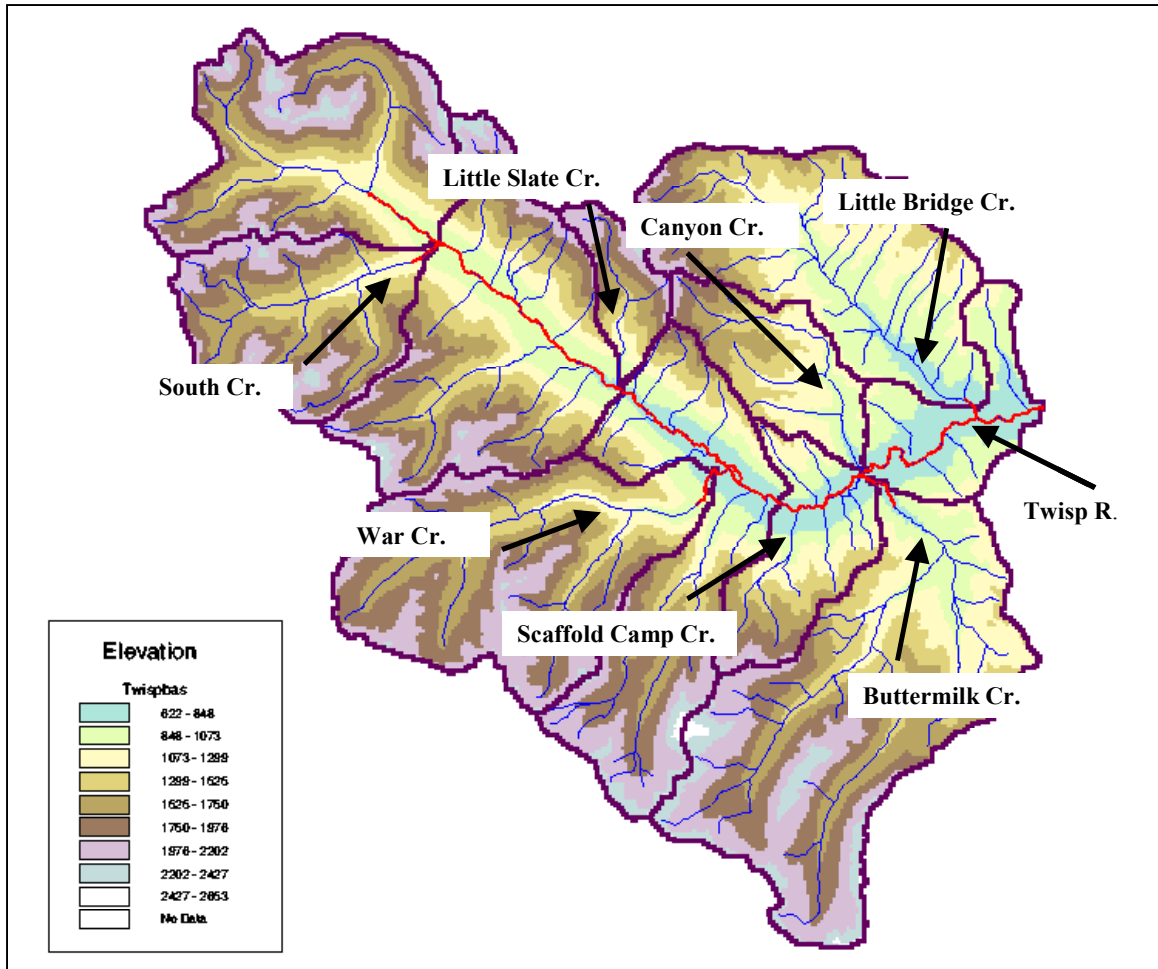
Figure 4.5: Twisp River Subbasin Delineations. The red line indicates the extent of anadramous fish populations (courtesy of Streamnet web page).

CHAPTER 5: LOW FLOW PREDICTION

5.1   REGIONAL REGRESSION MODEL

The purpose of the regional regression analysis is to estimate relationships between basin characteristics and the 7Q10s for the gaged basins. These relationships provide the basis for prediction of 7Q10's for ungaged stream reaches, and subsequently associated stream temperatures. One consideration in selection of candidate basin characteristics was that they should be extractable from GIS data bases – e.g., precipitation, characteristics like slope and aspect that are derivable from DEMs, vegetation, and similar attributes. The candidate characteristics that were evaluated are drainage area, average annual precipitation, total flow length in the basin, main channel slope and gage station elevation. Simple and multiple linear regression models were developed and compared using the Generalized Least Squares (GLS) method (Tasker and Stedinger, 1989).

The average annual and monthly precipitation values for the reference period 1961-1990) were obtained from a 4 km data set produced using the Parameter-elevation Regressions on Independent Slopes Model (PRISM) described by Daly et al. (1997). The data were provided courtesy of the Oregon Climate Service (http://www.ocs.orst.edu). Basin average precipitation was obtained by overlaying the PRISM precipitation and delineated basin GIS layers. Figure 5.1 shows the annual precipitation layer.
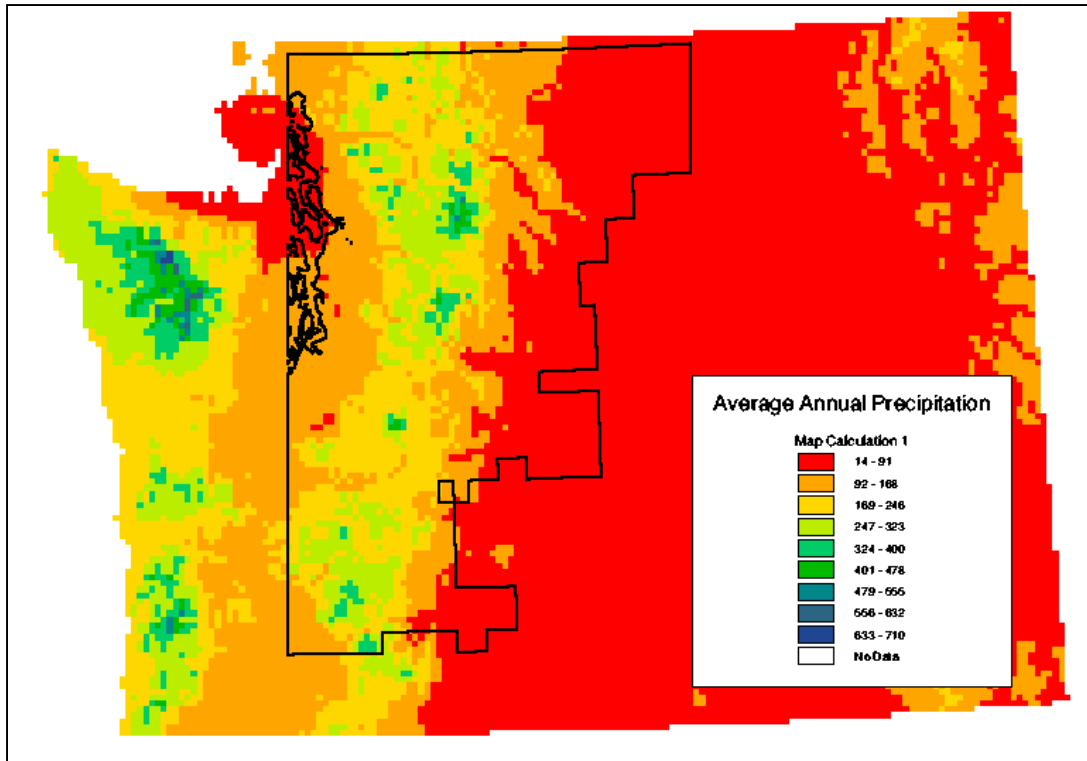
Figure 5.1: Average Annual Precipitation in centimeters (1961-1990) from the Oregon Climate Service (http://www.ocs.orst.edu).

The total flow length for each basin was extracted from the NHD hydrography data set discussed in Chapter 4. The length of the main channel and elevation of the upstream and downstream termini of the main channels were obtained from the 30 meter DEM and the NHD hydrography data sets, from which an average main channel slope was extracted.

The regional regression model is intended for use within the region(s) for which the parameters were estimated, and (at least roughly) within the ranges of the predictor attributes. Therefore, applicability is restricted to perennial streams with drainage areas less than about 1500 km^2. On this basis, the "training" data set for the regional regression models included 50 stations on the west side of the Cascade Mountains and 12 on the east side. The Generalized Least Squares method was chosen instead of the more

commonly used Ordinary Least Squares method (Helsel and Hirsch, 1992) because two assumptions of the OLS method are likely to be violated. The two assumptions are:

1.   The variance of the residuals ε is constant (homoscedastic).

2.   The residuals are independent.

Homoscedasticity is likely to be violated because the variances of the residuals will be lower for stations with longer record lengths. Independence of the residuals may be violated because discharges at the different gaging stations may be correlated as a function of their separation distance (Hirsch et al., 1993) .

Violation of homoscedasticity can be addressed through use of weighted least squares (Helsel and Hirsch, 1992). Temporal and/or spatial correlation can be addressed through use of a more general method (of which weighted least squares is a special case) known as Generalized Least Squares (GLS). GLS weights the squared residual by a factor that reflects the difference in record lengths and correlation between gages. The squares of the weighted residuals are then minimized (Hirsch et al., 1993; Helsel and Hirsch, 1992).

5.2   GENERALIZED LEAST SQUARES METHOD

The GLS regression analysis was performed using the USGS Generalized Least Squares Network Analysis (GLSNET) software (USGS, 1998). The procedure is based on the estimation techniques developed by Tasker and Stedinger (Tasker and Stedinger, 1985; Tasker and Stedinger, 1989) and is an extension of linear multivariate regression procedures. The model has the following form (Tasker and Stedinger, 1989).

$$\widetilde{Y} = X\beta + e$$

where

$\widetilde{Y}$ is a (n x 1) vector of 7Q10 values at n sites

X is a (n x p) matrix of (p-1) basin characteristics with a column of one's

β is a (p x 1) vector of regression parameters

e is a (n x 1) vector of random errors.

The initial p explanatory values in this analysis were chosen based on parameters that have been evaluated in low flow analyses in the past and can be obtained from the DEM. These parameters are latitude, longitude, drainage area, average precipitation depth over the catchment, main channel slope, average basin elevation and total length. Parameters not statistically significant were eliminated through a stepwise procedure where one parameter is eliminated at a time (Helsel and Hirschel, 1992; Draper and Smith, 1981).

The GLSNET program calculates the 7Q10 low flow from the 7-day low flow for each year assuming a Log Pearson Type III distribution. GLSNET uses an analysis of residuals technique (Tasker and Stedinger, 1985; Tasker and Stedinger, 1989) to estimate a regional regression equation to predict flow characteristics at ungaged sites. The technique assigns different weights (creates a weighting matrix) to observed flow characteristics based on record length, cross correlation with flow characteristics at other sites and an assumed model error structure.

5.3   RESULTS

The initial candidate explanatory variables were latitude, longitude, drainage area, average precipitation depth over the catchment, main channel slope, average basin elevation and total length. Parameters were eliminated using the t-test, PRESS (Prediction Error Sum of Squares) statistic and adjusted R^2 value (Helsel and Hirsch, 1992).

41

The t-test is used to determine whether the slope of the line is significantly different from zero (Helsel and Hirsch, 1992). The null hypothesis has the following form. $H_0 : \beta_1 = 0$ where β_1 is the slope of the regression line. The null hypothesis is rejected if the t statistic is greater than the critical value for t. The critical value is determined from the t-distribution based on the number of degrees of freedom minus 2. A detailed description of the use of the t-test for the situation represented here is given in Helsel and Hirsch (1992).

The PRESS statistic is the sum of the squared prediction errors and determines the error in making future predictions (Helsel and Hirsch, 1992). A minimum PRESS value produces the model with the least amount of error in predicting future values. The PRESS statistic is

$$PRESS = \sum_{i=1}^{n} e(i)^2$$

where,

$e(i)$ is the prediction residual

n is the number of observations

The adjusted R^2 value is the fraction of the variance explained by regression adjusted for the number of explanatory parameters (Helsel and Hirsch, 1992). The adjusted R^2 is

$$R^2{}_a = 1 - \frac{(n-1)SSE}{(n-p)SS_y}$$

where,

n is the number of observations

p is the number of model coefficients

SSE is the sum of squares of the residuals

SS_y is the sum of squares of the observations y

The model with the largest adjusted R^2 explains the largest fraction of variation of the data. The analysis was done by starting with all seven variables and then eliminating a variables based on the p-values where the p-values are the probability of obtaining the computed test statistic T at a significance level of 0.05 (details are in Helsel and Hirsch, 1992). The t–test results are given in the Tables 5.1 and 5.2.

The t statistics and p values for the first regression analysis with all seven parameters are listed in Table 5.1.

Table 5.1: 7Q10 Low Flow Regression Model Results with Seven Explanatory Variables.

Model Parameter	t statistic	p-value (alpha =0.05)
Drainage Area	3.64	0.0006
Longitude	0.02	0.985
Latitude	1.01	0.316
Precipitation	1.88	0.065
Main Channel Slope	3.63	0.0006
Average Basin Elevation	0.32	0.750
Total Stream Length	-0.79	0.436

Based on the p-values from the 7-parameter regression model, longitude, latitude, average basin elevation and total stream length were removed from the model. A regression model was developed with the remaining variables, with the p-values and t statistic presented in Table 5.2.

Table 5.2: Regression Model Results with Three Explanatory Variables.

Model Parameter	t statistic	p-value (alpha =0.05)
Drainage Area	14.36	0.0001
Precipitation	2.13	0.0374
Main Channel Slope	5.30	0.0001

A t-test was conducted to determine if the three parameter model has more explanatory power than a two parameter model. Since drainage area is the most significant predictor variable a comparison was also done between a one parameter model with area and the two parameter models of area,slope and area, precipitation. The null hypothesis of the test is that the slope coefficient of the additional parameter is zero, meaning that the parameter has no significance in the regression model. The results are presented in Table 5.3.

Table 5.3: Comparison of t-test Results for the 7Q10 Low Flow Regression Models with 1 to 3 Explanatory Variables.

Model Parameters	Additional Parameter Evaluated	t statistic (2)	p-value (alpha=0.05)
Area, Precipitation, Slope	Precipitation	2.1	0.0374
Area, Precipitation, Slope	Slope	5.3	0.0001
Area, Slope	Slope	5.5	0.0001
Area, Precipitation	Precipitation	2.4	0.0202

Based on the results, the additional parameters are adding explanatory power to the regression model, although precipitation is close to the border of being rejected. A smaller p-value indicates a stronger correlation between the model parameter and flow.

The null hypothesis (Ho) is rejected if the t statistic is less than the critical value of t, which is 2.

The models were evaluated for multicollinearity. Multicollinearity occurs when one or more of the explanatory variables are closely related to another. According to Helsel and Hirsch (1992), the variance inflation factor (VIF) is a good measure of multicollinearity. The VIF is defined as follows.

$$VIF_j = 1/(1 - R_j^2)$$

where R_j^2 is the coefficient of determination of the regression model with the jth variable as a function of the other explanatory variables in the model. The VIF was determined for both the slope and precipitation with the results presented in Table 5.4.

Table 5.4: Multicollinearity Results for the Area, Slope and Precipitation Explanatory Variables.

Response Variable	Explanatory Variable	VIF	R^2
Area	Slope	1.1	0.096
Area	Precipitation	1.0	0.021
Slope	Precipitation	1.0	0.004

A VIF close to 1 corresponds to a coefficient of determination of 0, indicating that the explanatory variables are not significantly related. Since all of the parameters are significant according the the t-test and multicollinearity is not a problem, two other measures, the adjusted R^2 value and the PRESS statistic, were evaluated to determine which regression model is the "best".

The PRESS statistic and adjusted R^2 results are given in Table 5.5.

Table 5.5 Comparison of PRESS statistics and adjusted R^2 values

Model Parameters	PRESS statistic	R_a^2	p-values (alpha=0.05)
Area	5.64	0.78	0.0001
Slope			0.0374
Precipitation			0.0001
Area	7.93	0.67	0.0001
Precipitation			0.0202
Area	5.60	0.76	0.0001
Slope			0.0001
Area	8.36	0.64	0.0001

The model with the minimum PRESS statistic is the model that predicts future values with the least amount of error. The model with the highest adjusted R^2 value has the smallest mean squared error. According to the results in Table 5.3, the regression models with slope and area and slope, area and precipitation as explanatory variables are the "best" with the model containing area and precipitation also performing well.

Although the regression models containing main channel slope seem to be the best choice, main channel slope is not extracted from the GIS-STRTEMP model easily and considerable data manipulation is required to determine the main channel length. Based on these results, therefore, the model with drainage area and precipitation as explanatory variables was chosen to predict 7Q10 low flow in the GIS-STRTEMP model. The regression model to predict 7Q10 low flow is given below.

$$\log10(7Q10\,flow) = 1.4157 + 1.06257(\log10\,area) + 0.95125(\log10(precip))$$

To verify that the regression model is valid for both the east and west side of the Cascade Mountains the predicted 7Q10 low flow was plotted against the residuals (Figure 5.1). A plot of the predicted variable against the residuals can be used to determine if any trends

exist in the variance which would indicate that the west and east side data can not be lumped into one model. From the plot in Figure 5.1 the west side and east side residuals seem to be intermixed, suggesting that a single model is adequate.
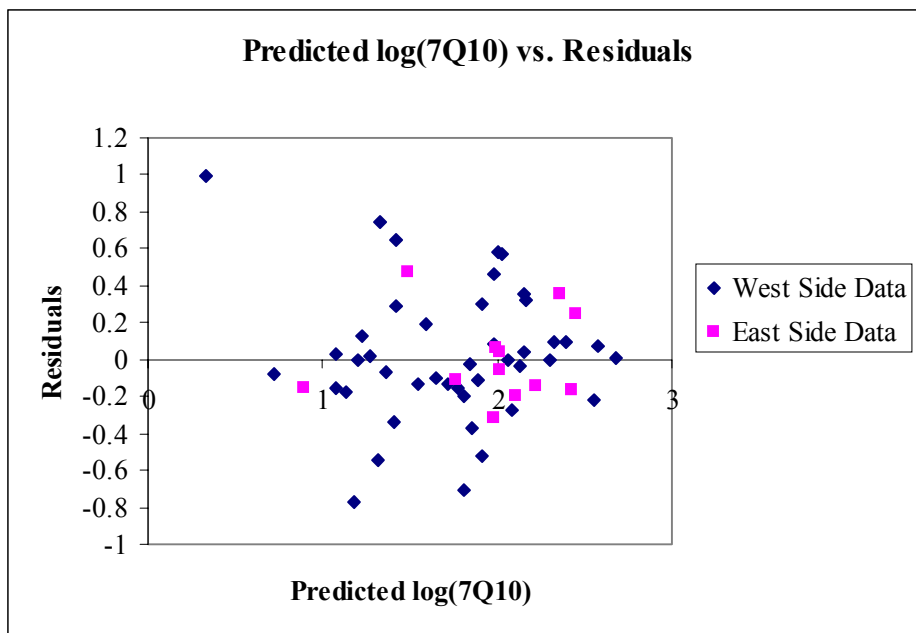
Figure 5.2. Plot of the Predicted log(7Q10) versus the Residuals.

Figures 5.3 and 5.4 show predicted 7Q10 flows for the Suiattle River basin on the west side of the Cascades and the Twisp River Basin on the east side of the Cascades, respectively. The expected behavior in a Cascade region watershed is flow decreasing with decreasing drainage area but also increasing with higher precipitation. In general, drainage area increases and precipitation decreases with declining elevation.   As the figures below show, both the Suiattle and Twisp basins follow the expected trend.
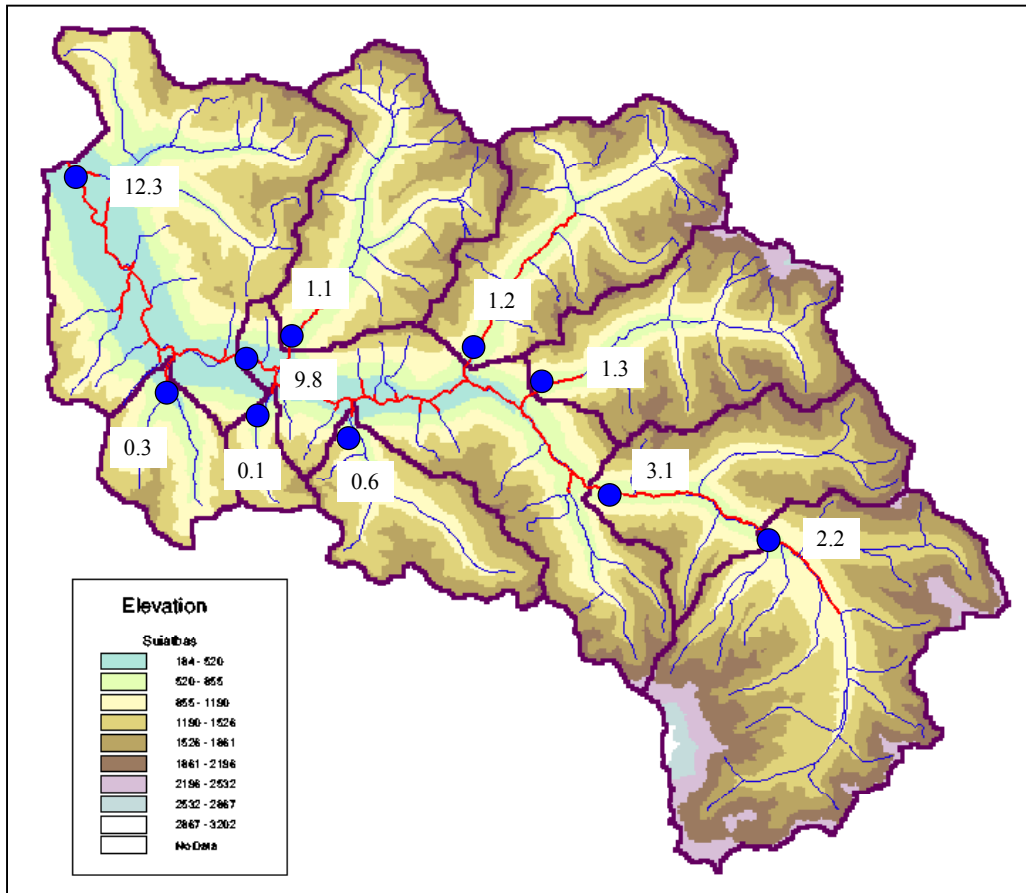
Figure 5.3: Predicted 7Q10 Flows (cms) for the Suiattle River Basin. Located on the West Side of the Cascades.
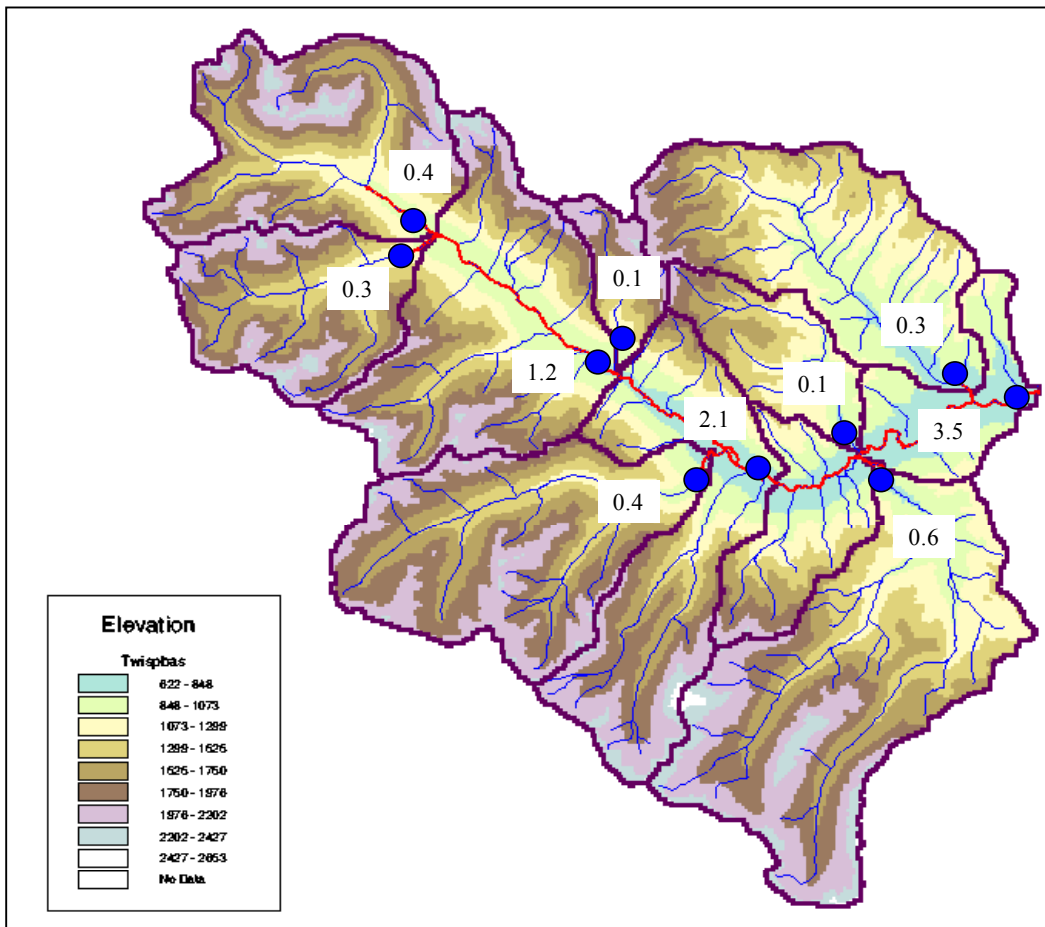
Figure 5.4: Predicted 7Q10 Flows (cms) for the Twisp River Basin. Located on the East Side of the Cascades.

CHAPTER 6: THE GIS-STRTEMP MODEL

The GIS-STRTEMP Model has three components: GIS,, solar radiation and energy balance. The GIS model allows the user to select a stream reach of interest and then extracts the relevant information (for example, drainage area, stream azimuth and slope aspect) for input into the solar radiation and energy balance. It consists of a 100-meter Digital Elevation Model (DEM) aggregated from a 10-meter DEM processed by Harvey Greenburg (Department of Geological Sciences, University of Washington) which in turn is derived from USGS topographic data. The DEM covers both the east and west slopes of the Washington Cascades as discussed in Chapter 5. The DEM was clipped into separate DEM's for each hydrologic unit code (HUC). This was done to reduce the model run time and to allow the user to locate stream reaches of interest more easily. To use the model, the user selects the HUC within which the stream reach of interest is located, and then selects the reach. The user is then prompted to enter the riparian vegetation parameters used in the solar radiation component of the GIS-STRTEMP model.

The solar radiation and energy balance models are a modified version of the STRTEMP model of LaMarche et al (1997). The STRTEMP model is based on a modified version of the SOLARFLUX radiation model (Rich et al., 1994) and an energy balance finite difference program. The main modifications to the original STRTEMP model of LaMarche et. al were to integrate the GIS, solar radiation and energy balance models into one program and to estimate many of the parameters that were required as user input in the original model. The specific input parameters are discussed below.

6.1   SOLAR RADIATION MODEL

6.1.1   MODEL DESCRIPTION

The incoming direct solar radiation is calculated using a modified version of the SOLARFLUX model (Rich et al., 1994). The modified SOLARFLUX model calculates incoming radiation based on surface orientation, solar angle, shadowing due to topographic features and riparian vegetation and atmospheric attenuation. In the solar radiation model the total direct radiation is calculated by first accounting for topographic influences and then riparian vegetative influences. The model starts at the upstream end of the reach and moves downstream incrementally based on the latitude, longitude, stream azimuth angle and number of cells in the reach.

Direct Beam Calculation for Topography

Direct beam radiation is calculated based on the shadow patterns across the DEM at each time step (hourly) and the angle of incidence of direct radiation reaching each surface location that is not in shadow for each time step (Rich et al., 1994).

The direct beam component due to topographic influences is calculated using the following equation (Monteith and Unsworth, 1990, Chapter 5)

$$I_{direct} = \tau S_0 \left(\sin(slope) \cos(\varphi) \cos(\theta_{sun} - aspect) + \cos(slope) \sin(\varphi) \right)$$

where,

τ is the atmospheric transmissivity

S_0 is the solar constant

slope is the angle of the earth's surface from a horizontal plane

φ is the solar illumination angle above the horizon

θ_{sun} is the angle of sun relative to north (solar aspect)

aspect is the downslope direction of the maximum rate of change in elevation

relative to north

The slope aspect and solar aspect are depicted in Figure 6.1.
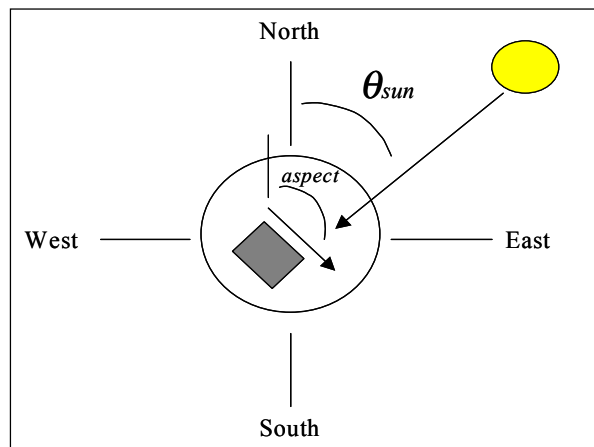
Figure 6.1: Depiction of the slope aspect and solar aspect in the direct beam calculation.

The solar illumination angle and topographic slope are depicted in Figure 6.2.
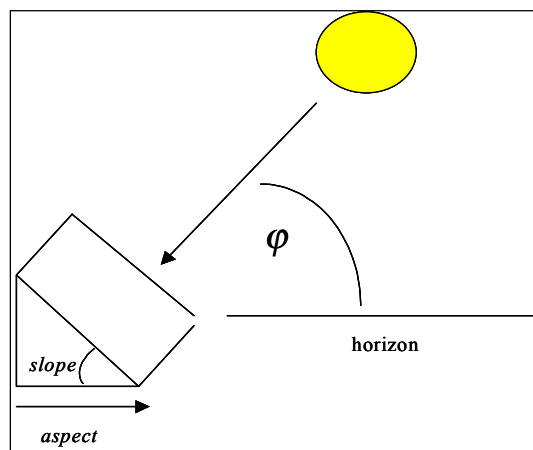
Figure 6.2: Depiction of the solar illumination angle and topographic slope in the direct beam calculation.

Direct Beam Calculation for Riparian Vegetation

The SOLARFLUX model was modified to take into account the effects of riparian vegetation on the incoming solar radiation reaching the surface of the stream. The direct beam radiation calculated for topography is used to calculate the effects of the vegetative canopy on the direct beam solar radiation that reaches the stream. The incoming direct beam radiation is partitioned into three sections based on the fraction of the canopy through which light travels before reaching the stream surface, as depicted in Figure 6.3.
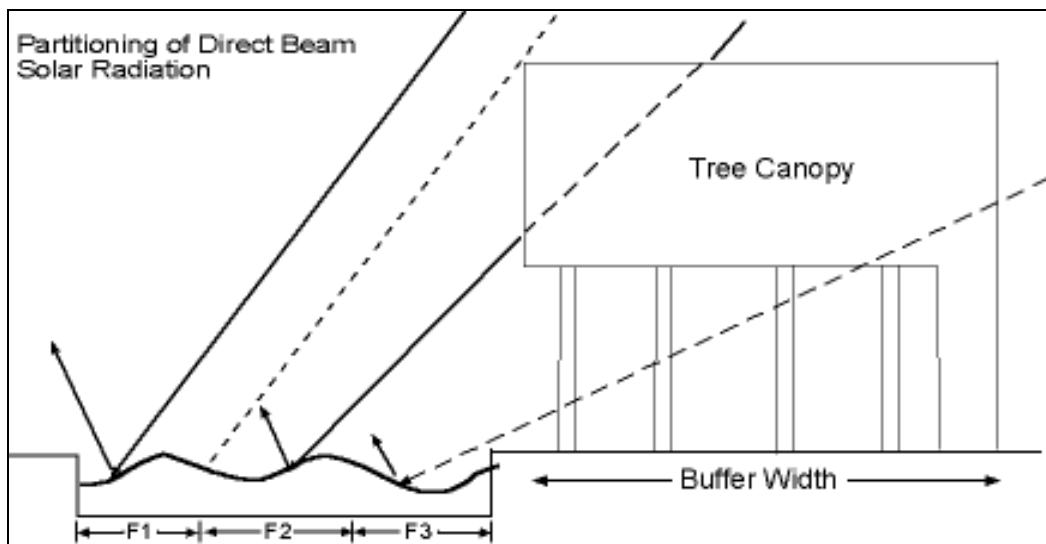
Figure 6.3: Vegetative partitioning of incoming direct beam solar radiation (from LaMarche et al., 1997).

The direct beam radiation component due to the vegetative canopy is calculated from Beer's Law (Monteith and Unsworth, 1990) as follows:

$$I_{direct} = I_0 \exp(-k \cdot LAI)$$

where,

I_0 is the direct beam radiation calculated for the topographic influences.

k is the coefficient of attenuation

LAI is the leaf area index

In the modified SOLARFLUX model, k varies from 0.2 to 0.5 depending on the path length of light through the canopy. For small buffers with path lengths at low angles a coefficient between 0.1 and 0.35 is used (LaMarche et al., 1997).

The leaf area index (LAI) is the projected (one-sided) area of leaves per unit of ground surface (Campbell and Norman, 1997). LAI varies depending on age and type of vegetation. LAI values can range from 1.5 for some stands of Lodgepole Pine to over 13 for some stands of Douglas Fir (Buchmann et al., 1997; Thomas and Winner, 2000). The user must select a representative LAI value for the stream reach of interest. In the simulations for the Suiattle and Twisp River basins LAI values of 8 and 5 were used, respectively. Typical values of LAI from the literature for more common species found in the Cascades are provided in a pulldown menu in the GIS-STRTEMP model.

When the direct beam solar radiation has been calculated by the modified SOLARFLUX model, it is saved for subsequent use as an input variable in the energy balance finite difference program.

6.1.2   MODEL INPUT PARAMETERS

The following parameters are determined within the GIS-STRTEMP model. Most of these parameters were required as user inputs in the original STRTEMP model:

Julian Day, Local Start and End Time and Incremental Interval – The julian day is set at 208 (July 27th) which corresponds to the average day that experiences the maximum 10

year air temperature. The local start and end time are set to span a 24 hour period with an incremental interval of 1 hour.

Latitude and Longitude – The latitude and longitude are obtained from the DEM and correspond to the location of the upstream end of the reach.

Stream Azimuth Angle – The stream azimuth angle is a constant and is obtained from the stream network coverage. It is the average azimuth of the reach. The model moves incrementally along the stream reach based on the stream azimuth.

Number of Cells in Stream Reach – The number of cells in the stream reach are determined by the length of the stream reach divided by the cell size (100 meters). The stream length is the straight distance between the upstream and downstream ends of the reach. The model steps through the stream reach based on the number of cells, the stream azimuth and the latitude and longitude. It begins at the upstream cell and increments to the next downstream cell using the stream azimuth and beginning latitude and longitude.

Transmissivity – The atmospheric transmissivity is the fraction of the solar radiation transmitted through the atmosphere (Dingman, 1994, Appendix E). It varies throughout the year, and is a function of atmospheric constituents such as dust, oxygen, and water vapor (Bristow and Campbell, 1984). A constant transmissivity of 0.70 is used in the GIS-STRTEMP model. Bristow and Campbell (1984), determined a clear sky transmissivity for Seattle/Tacoma and Pullman of 0.72 and 0.70, respectively. Calculation of the total transmissivity (per an empirical relationship discussed in Bristow and Campbell for the Entiat and Beckler field sites resulted in an average total transmissivity of 0.70. Based on these results, and the consideration that the computations pertain to mid- summer conditions when air temperatures are maximum and cloud cover is minimum, a transmissivity value of 0.70 was chosen. This is a fixed value for all computations.

Stream Width – The stream width is the average wetted width of the stream reach. The stream width is estimated from regional regression relationships for the eastern and Western Cascades based on drainage basin area (Sullivan et al., 1990). The regression equations are as follows.

Western Cascades:

$$Depth = 0.1625 * \log 10 (DrainageArea) + 0.061$$

Eastern Cascades:

$$Depth = 0.1484 * \log 10 (DrainageArea) + 0.011$$

where depth is stream depth in meters and drainage area is in square kilometers. The R-squared values are 0.50 and 0.95, respectively.

The parameter values are stored in a text file which is accessed by the GIS-STRTEMP model based on the reach selected by the user.

6.1.3   USER INPUT PARAMETERS

The GIS-STRTEMP model requires the user to provide the riparian vegetation parameters. This allows the user to model changes in riparian vegetation and buffer width. The riparian parameters are.

Average Tree Height – The average height of the streamside vegetation.

Average Canopy Height – The average height of the bottom of the canopy.

Bank to Canopy Distance – The average distance from the stream bank to the canopy.

Buffer Width – The average buffer width adjacent to the stream.

56

Leaf Area Index (LAI) - The leaf area index is the area of the canopy projected onto the ground surface.

6.2   ENERGY BALANCE MODEL

6.2.1   MODEL DESCRIPTION

The energy balance component of the GIS-STRTEMP model solves the energy balance of a stream reach with a finite difference explicit numerical method. Each cell in the stream reach represents a control volume, as depicted in Figure 6.4.
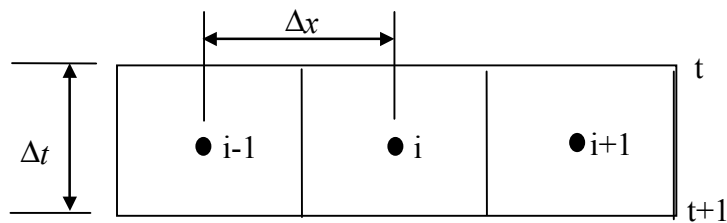
Figure 6.4: **Stream reach represented as a series of control volumes (from LaMarche et al., 1997).**

As discussed in Section 1.1, the equation for the energy balance of a stream reach in its one–dimensional state with a constant cross sectional area is:

$$\frac{\partial T}{\partial t} + v\frac{\partial T}{\partial x} = \frac{E}{c_p \rho d}$$

where,

   d is depth

   ρ is water density.

The finite approximation of the energy equation for cell i is expressed as (LaMarche et al., 1997):

$$\frac{T_i^{t+1} - T_i^t}{\Delta t} + v \frac{T_{i+1}^t - T_{i-1}^t}{2\Delta x} = \frac{E_i^{t+1} + E_i^t}{2\rho c_p}$$

Solving it terms of temperature at time t+1 for node i gives:

$$T_i^{t+1} = T_i^t - \Delta t \frac{Q_i}{A_c} \frac{T_{i+1}^t - T_{i-1}^t}{2\Delta x} + \Delta t \frac{E_i^{t+1} + E_i^t}{2\rho c_p}$$

Equations to Estimate The Energy Transfer Terms:

The energy exchange between the stream and its environment is a function of incoming and reflected short wave radiation, incoming long wave radiation from the sky and riparian canopy; emitted long wave from the stream, convective heat exchange between water and air; evaporation and condensation between the air/stream interface and advection from groundwater gains or losses. The physics of stream heating is discussed in detail in Section 1.1.

Net Short Wave Radiation - The net short wave radiation is calculated in the solar radiation component of the model and takes into account the influences of topography and riparian vegetation.

Net Long Wave Radiation – The net long wave radiation is the difference between incoming long wave from the sky and vegetation, and outgoing long wave emitted from the stream, and is estimated by:

$$L_n = L_{air} + L_{tree} - L_{water}$$

$$L_n = \sigma\left[(e_a + e_t)T_a^4 - e_w T_w^4\right]$$

where,

σ is the Stefan Boltzman constant

T_a air temperature

T_w water temperature

e_a is the emissivity of water

e_a is the emissivity of air

$$e_a = e_{ac}(1 + .17(CL^2))$$

where,

e_{ac} is the emissivity of air without cloud cover given by,

$$e_{ac} = 1 - .261\exp(-7.5x10^{-5}xT_a^{-4}) \text{ (Shuttleworth, 1993)}$$

CL is the percentage of cloud cover.

Advection – Advection is the heat gain or loss from groundwater, calculated by:

$$A = \rho C_p Q_g (T_g - T_w)$$

The density of water is ρ, C_p = specific heat of water at constant pressure, Q_g = ground water flow, and T_g and T_w are the groundwater and stream water temperatures respectively.

Evaporation/Condensation – The evaporation and condensation estimates are based on the Penman equation for potential evaporation from a shallow free water surface (Shuttleworth, 1993).

$$E_p = \frac{\Delta}{\Delta + \gamma}(R_n + A_h) + \frac{\gamma}{\Delta + \gamma}\frac{6.43(1+.536U_2)D}{\lambda} \quad \text{(mm/day)}$$

where,

Δ is the gradient of the function $e_s(T)$ (change in vapor pressure/change in temperature) given by: $\Delta = \frac{4098e_s}{(237.3+T)^2}$

e_s is the saturated vapor pressure $= .6108 \exp\left(\frac{17.27T}{(237.3+T)}\right)$ (kPa/°C).

γ is the psychrometric constant $= .0016286\frac{P}{\lambda}$ (kPa/°C).

λ is the latent heat of vaporization of water, given by: $\lambda = 2.501 - .002361T_a$ (MJ/Kg).

U is wind speed at two meters (m/s).

D is vapor pressure deficit, e_s-e , in kPa.

R_n is the net radiation at the free water surface

A_h is the advected energy.

Convective Heat Exchange - The convective heat exchange between the air water surface is estimated using (Raphael, 1962):

$$C = .0124 \cdot U \cdot P(T_w - T_a)$$

where U (m/s) is wind speed, P (kPa) is atmospheric pressure, and T_w and T_a are the water and air temperatures (°C), respectively.

6.2.2   MODEL INPUT PARAMETERS

The following parameters, required as user inputs in the original STRTEMP model (LaMarche et al., 1997) are determined within the GIS-STRTEMP.

Hourly Air Temperature– The hourly air temperature time series is produced from the 10 year maximum and the minimum daily air temperature. First, the 10 year maximum air daily temperature is split into 3 hour intervals (Anderson, 1968) and then hourly values are interpolated from the 3 hourly values.

The 10 year maximum air temperature was determined from historical air temperature data. A normal probability distribution was fit to data from air temperature stations in Washington State with 10 or more years of data. The SYMAP algorithm (Gaile and Millmott, eds., 1984) was used to grid the air temperature data with the air temperature adjusted for the lapse rate. The average date of maximum air temperature was July 27th. Therefore this day was chosen to run the simulations. Figure 6.5 shows the 10 year maximum air temperature gridded over the study area.
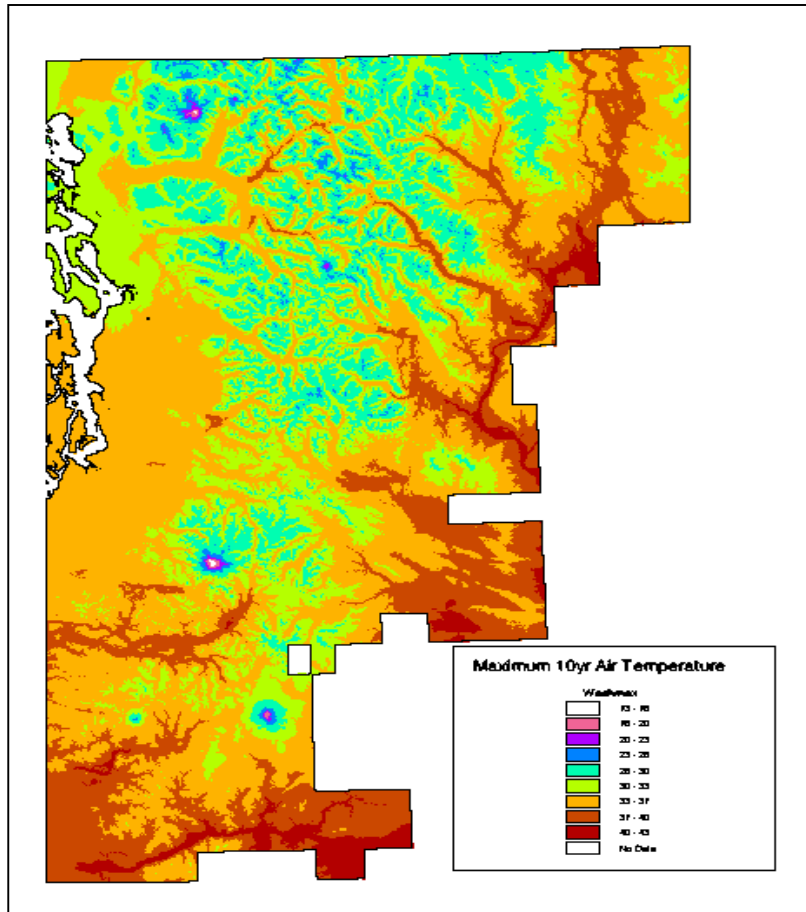
Figure 6.5: 10 Year Gridded Maximum Air Temperatures.

Minimum Daily Air Temperature – The minimum daily air temperature was estimated
for the days on which the maximum daily air temperature occurred for each year of the
record. A normal probability distribution was fit to these data and the 10 year return
period value was obtained. The data were then gridded following the same procedure as
for the maximum 10 year daily temperature. Figure 6.6 shows the 10 year minimum air
temperature gridded over the study area.
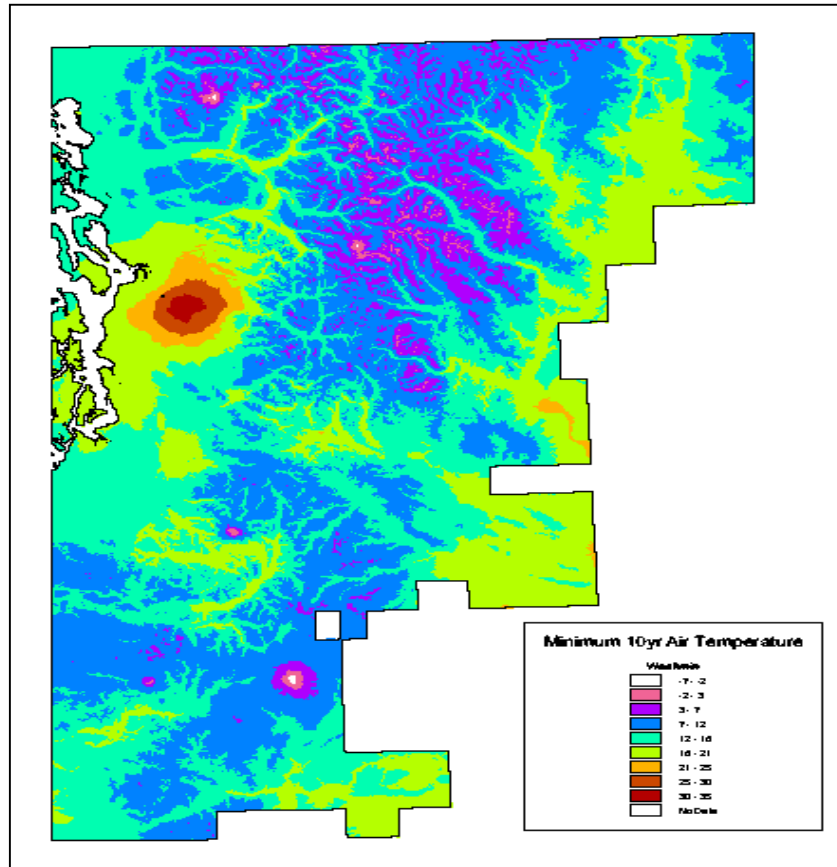
Figure 6.6: 10 Year Gridded Minimum Air Temperatures.

Hourly Shortwave Solar Radiation Timeseries – hourly net incoming radiation files from the solar radiation component of the model.

Daily Cloudy Cover Time Series – The cloud cover was assumed to be 1 minus the transmissivity which is 30%.

Mean Annual Air Temperature – The mean annual air temperature is approximated as the average of the daily historical maximum and minimum air temperature values. Figure 6.7 shows the gridded average annual air temperature values.
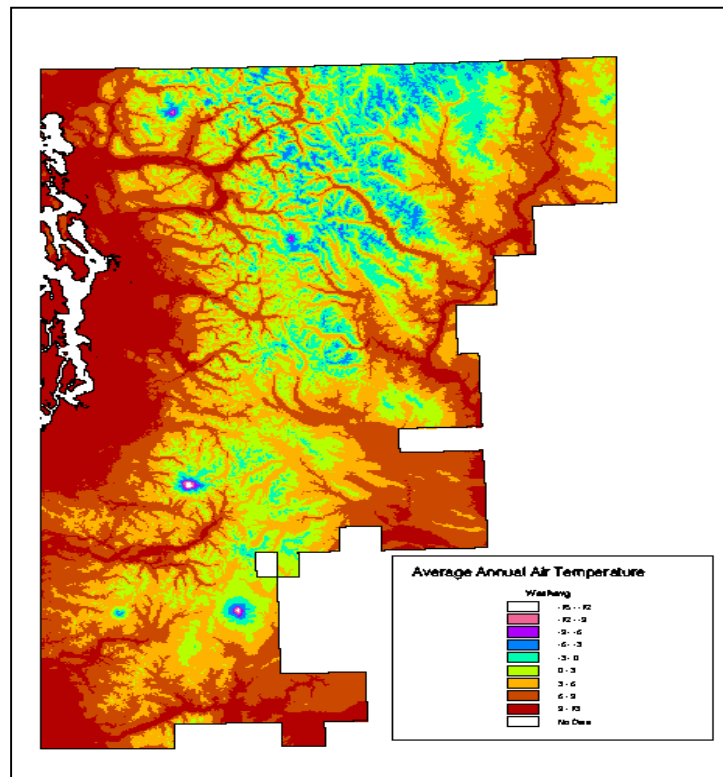
Figure 6.7: Gridded Average Annual Air Temperatures.

Reach Length - This is obtained from the DEM and is the straight line distance from the upstream and downstream ends of the reach.

Reach Inflow – This is obtained from the 7Q10 low flow regression relationship developed in Chapter 4.

Reach Outflow – The reach outflow is approximated as the reach inflow plus the groundwater inflow

Reach Average Stream Velocity – The reach average stream velocity is approximated using the reach inflow, estimated stream depth and width and assuming a rectangular channel shape.

64

Reach Average Width – The reach average width is the same value used in the solar radiation component of the model.

Reach Average Depth – The reach average depth is obtained from a regression relationship where depth is a function of basin area, developed by the TFW (Sullivan et al., 1990). The regression equation is as follows.

$$WettedWidth = 5.65*\log10(DrainageArea) - 2.51$$

where, the wetted width is in meters and the drainage area is in square kilometers. The R-squared value is 0.66.

Groundwater Inflow – The TFW found that the groundwater inflow varied in the summer from 0.004 to 0.065 m^3/s/km (Sullivan et al., 1990). The average value 0.007 m^3/s/km was used in the GIS-STRTEMP model.

Wind Speed – The historical average wind speed from Washington State stations were averaged for July 27th. The wind speed is assumed to be constant at 2.8 m/s.

Initial Water Temperature – The initial water temperature corresponds to the temperature at the upstream boundary of the reach. As discussed in LaMarche et al. (1997), the initial water temperature and reach length impacts the predicted water temperature and therefore, a stream reach greater than 1800 meters is needed to eliminate the influence of the initial starting temperature. In this study reach lengths vary from several hundred meters to several thousand meters. To eliminate the effect described above, the initial water temperature is obtained by simulating a reach 3000 meters long ending at the upstream boundary of the reach of interest with the characteristics of the upstream boundary of the reach. The water temperature simulated at the end of this reach is then used as the initial water temperature for the stream reach of interest.

CHAPTER 7: GIS-STRTEMP MODEL ANALYSES

7.1 MODEL CALIBRATION

7.1.1   Calibration Reaches

The GIS-STRTEMP was calibrated using field data collected in the summer of 2000 in the Beckler and Entiat River subbasins (see Chapter 3). Descriptions of the basins are also given in Chapter 3.

7.1.2   Calibration Results

The calibration results and plot are presented in Table 7.1 and Figure 7.1. The predicted water temperature was within 2 $°C$ of observations for all locations except for the Beckler upstream site and the Entiat downstream site.

Table 7.1. Calibration Results

Location	Measured and Predicted Daily Stream Temperatures (°C)					
	Average Daily		Minimum Daily		Maximum Daily	
	Measured	Predicted	Measured	Predicted	Measured	Predicted
Entiat - Upstream	8.4	9.9	6.8	8.2	9.8	11.0
Entiat - Midstream	9.7	10.5	8.1	8.9	11.5	11.6
Entiat - Dowstream	11.3	12.3	9.2	10.8	13.7	13.4
Beckler - Upstream	9.3	10.6	8.1	9.3	10.6	11.6
Beckler - Midstream	12.2	12.7	10.8	11.2	13.8	13.9
Beckler - Downstream	13.5	13.3	11.7	12.3	15.8	14.1

Location	Average Differences (°C): Measured - Predicted		
	Average Daily Temp	Minimum Daily Temp	Maximum Daily Temp
Entiat - Upstream	-1.5	-1.4	-1.1
Entiat - Midstream	-0.9	-0.8	-0.1
Entiat - Dowstream	-1.1	-1.7	0.2
Beckler - Upstream	-1.3	-1.2	-0.9
Beckler - Midstream	-0.5	-0.3	0.0
Beckler - Downstream	0.2	-0.6	1.8

7.2 MODEL SIMULATIONS

7.2.1   Simulated Stream Reaches

As discussed in Chapter 4, ten stream reaches from the Suiattle and ten from the Twisp
River basins were chosen to demonstrate the use of the GIS-STRTEMP model.
Simulations were performed for three buffer widths: 0, 16.4 meters (50 feet) and 65.6
meters (200 feet). The water temperature results with the varying buffer widths for the
Suiattle and Twisp River basins are shown in Tables 7.2 and 7.3, respectively. The
results are shown graphically in Figures 7.1 through 7.6.

Table 7.2: GIS-STRTEMP Simulation Results for the Suiattle River Basin

Description	Area (sq. km)	Stream Azimuth	Predicted Water Temperatures ($^\circ$C)		
			Buffer Width (meters)		
			0	16.4	65.6
d/s of Big Creek	852	276	24.6	23.9	23.9
Buck Creek	86	217	19.6	19.2	19.1
Downey Creek	91	208	20.1	19.7	19.6
Sulphur Creek	85	244	19.5	18.9	18.9
Straight Creek	30	193	20.1	19.8	19.6
u/s of Milk Creek	235	279	20.1	19.5	19.5
Lime Creek	46	276	18.6	18.0	18.0
d/s of Vista Creek	162	298	20.0	19.3	19.3
d/s of Circle Creek	669	226	22.3	21.9	21.8
Circle Creek	12	23	17.4	17.1	17.0

Table 7.3: GIS-STRTEMP Simulation Results for the Twisp River Basin

Description	Area (sq. km)	Stream Azimuth	Predicted Water Temperatures ($^\circ$C)		
			Buffer Width (meters)		
			0	16.4	65.6
u/s of Myer Creek	538	77	24.8	24.0	24.0
Buttermilk Creek	95	312	21.6	20.5	20.3
Little Bridge Creek	63	145	22.9	22.0	21.8
d/s of Little Slate Creek	180	120	9.3	8.3	8.3
War Creek	69	79	21.3	20.1	20.1
South Creek	40	68	20.8	19.5	19.5
Canyon Creek	23	157	20.2	19.4	18.9
u/s of South Creek	59	126	20.0	18.8	18.7
u/s of Scaffold Camp Creek	309	117	20.7	19.7	19.6
Little Slate Creek	11	181	24.1	23.1	22.5
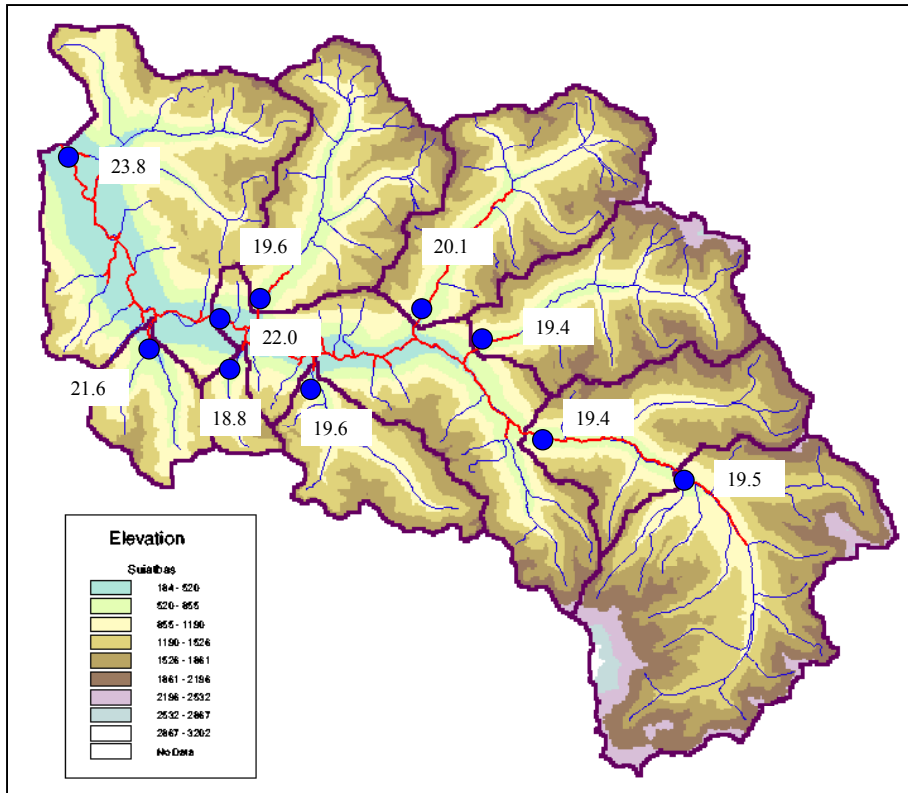
Figure 7.1: Water Temperature Results (°C) for the Suiattle River Basin with a Buffer Width of 0 meters.
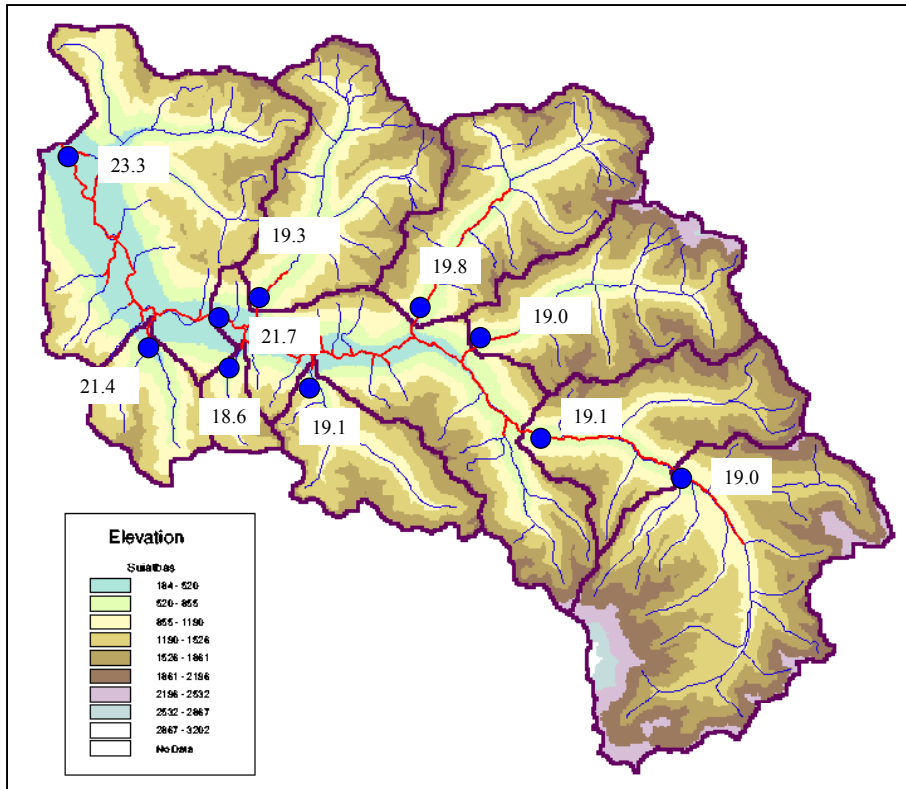
Figure 7.2: Water Temperature Results (°C) for the Suiattle River Basin with a Buffer Width of 16.4 meters (50 feet).
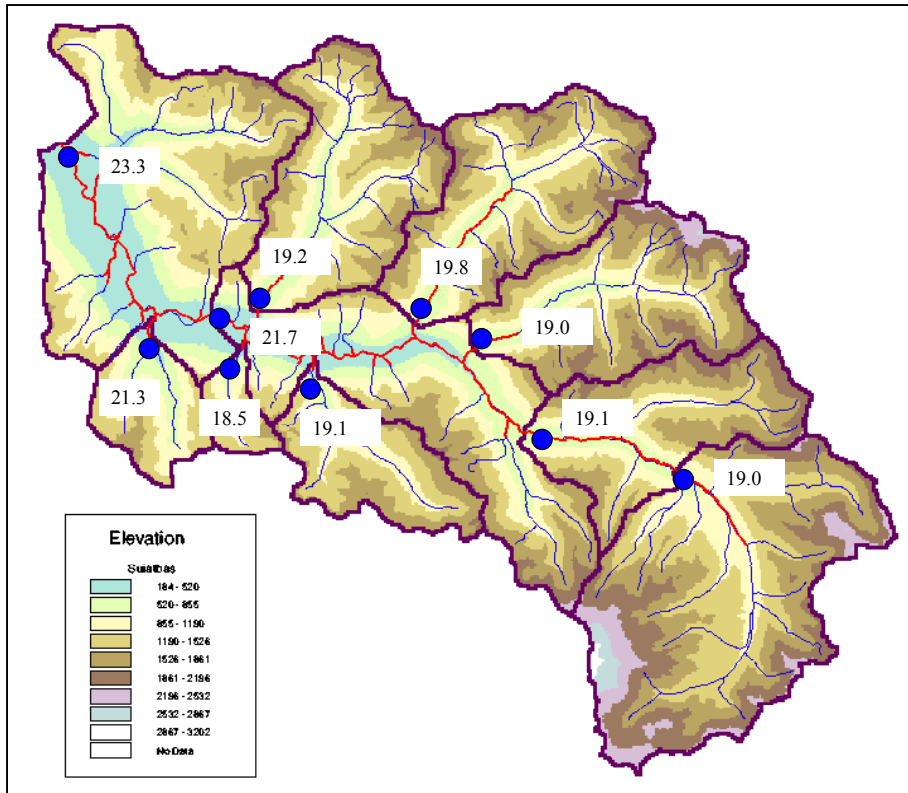
Figure 7.3: Water Temperature Results (°C) for the Suiattle River Basin with a Buffer Width of 65.6 meters (200 feet).
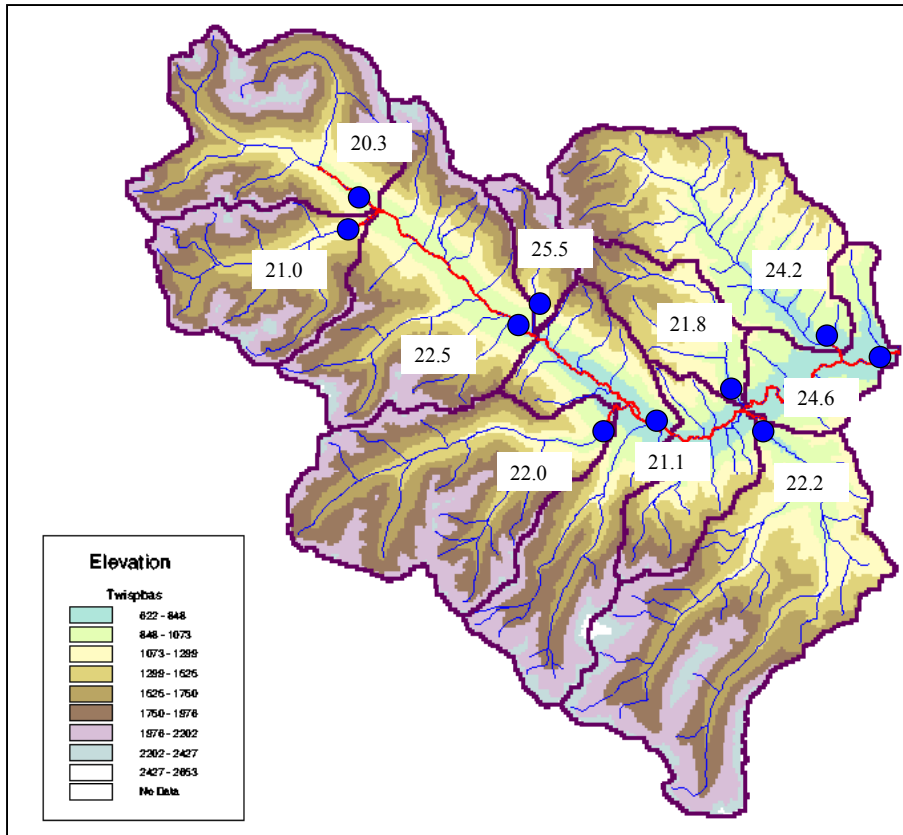
Figure 7.4: Water Temperature Results (°C) for the Twisp River Basin with a Buffer Width of 0 meters.

72
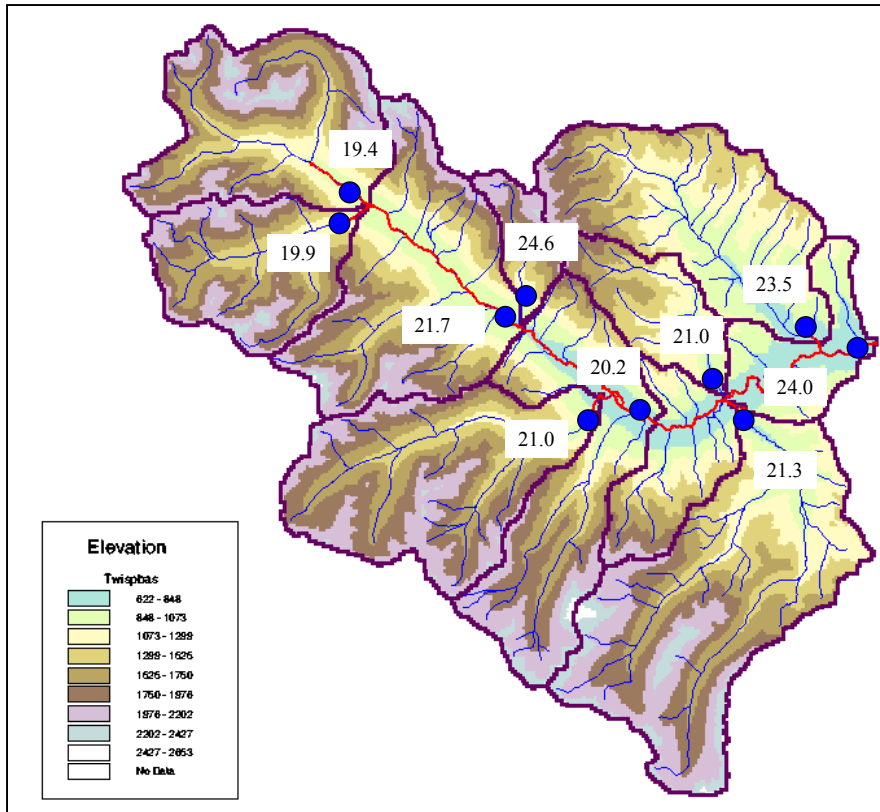
Figure 7.5: Water Temperature Results (°C) for the Twisp River Basin with a Buffer Width of 16.4 meters (50 feet).
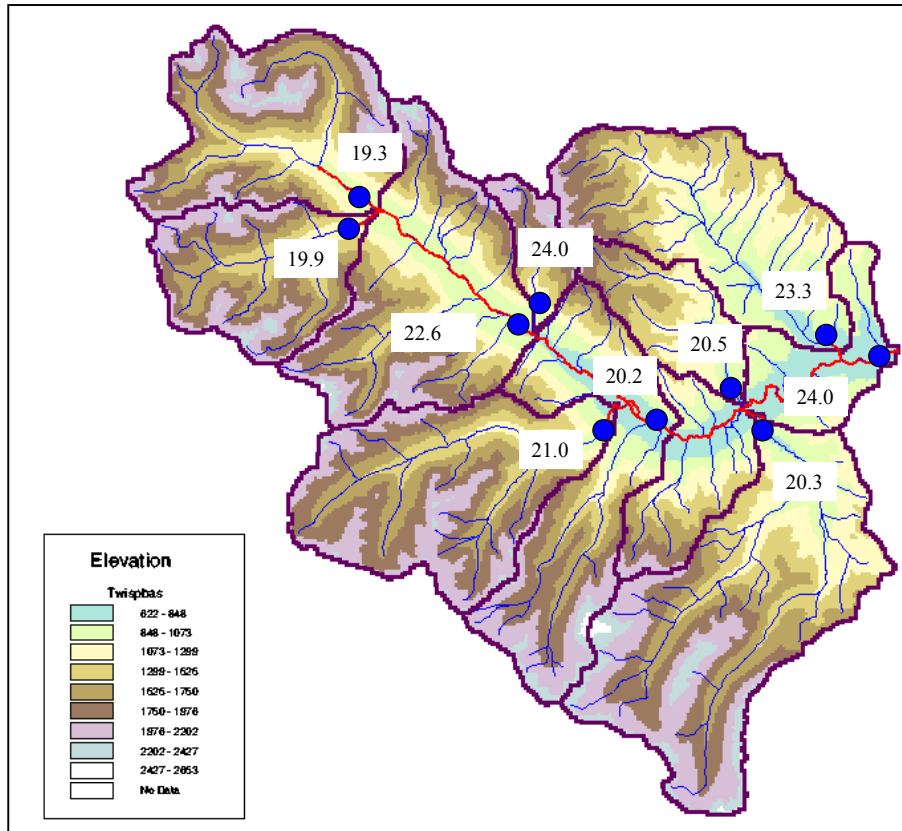
Figure 7.6: Water Temperature Results (°C) for the Twisp River Basin with a Buffer Width of 65.6 meters (200 feet).

In addition to the simulations performed for the Suiattle and Twisp River basins, 14 stream reaches with measured stream temperature data were chosen to compare against the GIS-STRTEMP model results. Sufficient stream temperature data do not exist to calibrate the predicted 10 year maximum stream temperatures with observed 10 year stream temperatures. Instead, the 10 year model results were compared with the maximum stream temperatures observed during the summers of 1988, 1999, and 2000 to show where the model results fall in relation to observed maximum summer temperatures. A description of the stream reaches is given in Table 7.4. The data were obtained from the TFW temperature study data appendix (Sullivan et.al, 1990), the USFS Entiat Ranger Station and field measurements from this study.

Table 7.4: Source of Temperature Data for Stream Reaches

Stream Reach	Description
Little Naches River	TFW Temperature Study, Summer 1988
Crow Creek	TFW Temperature Study, Summer 1988
Deer Creek Above DeForest	TFW Temperature Study, Summer 1988
Mad River Above Pine Flat Campground	USFS Entiat Ranger Station, Summer 1999
Hornet Creek	USFS Entiat Ranger Station, Summer 1999
Preston Creek	USFS Entiat Ranger Station, Summer 1999
Tillicum Creek	USFS Entiat Ranger Station, Summer 1999
Entiat River at River Mile 26	USFS Entiat Ranger Station, Summer 1999
Entiat River – Upstream Field Site	GIS-STRTEMP Study, Summer 2000
Entiat River – Midstream Field Site	GIS-STRTEMP Study, Summer 2000
Entiat River – Downstream Field Site	GIS-STRTEMP Study, Summer 2000
Beckler River – Upstream Field Site	GIS-STRTEMP Study, Summer 2000
Beckler River – Midstream Field Site	GIS-STRTEMP Study, Summer 2000
Beckler River – Downstream Field Site	GIS-STRTEMP Study, Summer 2000

7.2.2   Predicted Stream Temperatures

The GIS-STRTEMP model results and observed water temperatures are presented in Table 7.5.

Table 7.5: Comparison of Predicted 10 Year Water Temperatures with Observed Maximum Summer Temperatures.

Stream Reach	Predicted Maximum 10 Year Water Temperature (°C)	Measured Maximum Water Temperature (°C)
Little Naches River	21.8	17.5
Crow Creek	23.3	16.0
Deer Creek Above DeForest	20.4	20.5
Mad River Above Pine Flat Campground	18.3	17.9
Hornet Creek	21.0	17.2
Preston Creek	19.8	17.2
Tillicum Creek	18.7	17.2
Entiat River at River Mile 26	20.0	16.0
Entiat River – Upstream Field Site	16.9	12.0
Entiat River – Midstream Field Site	18.1	13.6
Entiat River – Downstream Field Site	20.1	16.0
Beckler River – Upstream Field Site	16.1	12.7
Beckler River – Midstream Field Site	18.4	16.0
Beckler River – Downstream Field Site	18.5	18.0

The predicted maximum 10 year stream temperatures are above the measured except for the Deer Creek above DeForest site. Insufficient data are available to determine the reason for this anomaly.

7.3 SENSITIVITY ANALYSIS

7.3.1 Model Parameters

A cursory sensitivity analysis was performed on a 1500 meter reach in the Entiat River basin to determine the change in the predicted stream temperature with a change in the model input parameters. The sensitivity analysis was performed by varying one parameter while holding all other parameters constant. The percent change in the

predicted stream temperature was then determined for each parameter. The parameters evaluated and the range over which they were varied is presented in Table 7.6.

Table 7.6: GIS-STRTEMP Parameters used in the Sensitivity Analysis.

GIS-STRTEMP Parameter	Range of Sensitivity Analysis
Groundwater Inflow (m^3/s/km)	0.002 to 0.025
7Q10 Flow (cubic meters/second)	0.1 to 1
Stream Depth (meters)	0.25 to 1.0
Stream Width (meters)	2 to 20
Stream Velocity (meters/second)	0.25 to 1
Initial Water Temperature ($°C$)	7 to 18
Average Annual Air Temperature ($°C$)	5 to 15
LAI	1 to 9
Avg Canopy Height (meters)	5 to 20
Avg Tree Height (meters)	5 to 30
Bank/Canopy Distance (meters)	0 to 100
Buffer Width (meters)	0 to 100

7.3.2   Sensitivity Analysis Results

The results from the sensitivity analysis are presented in Table 7.7.

Table 7.7: Sensitivity Analysis Results

GIS-STRTEMP Parameter	Water Temperature ($°C$)			
	Low	Middle	Middle	High
Groundwater Inflow (m^3/s/km) (0.002,0.0025)	20.6	-----	-----	20.6
7Q10 Flow (cms) (0.1, 10)	20.6	-----	-----	19.8
Stream Depth (m) (0.25, 1)	21.2	-----	-----	17.9
Stream Width (m) (2, 20)	18.3	-----	-----	21.4
Stream Velocity (m/s) (0.25, 1)	20.6	-----	-----	20.6
Initial Water Temperature ($°C$) (7, 13, 14, 18)	17.6	18.9	19.2	20.0
Average Annual Air Temperature ($°C$) (5,15)	19.8	-----	-----	21.3
LAI (2,4,7,17)	20.9	19.4	18.7	18.4
Avg Canopy Height (m) (5,20)	19.3			21.2
Avg Tree Height (m) (0,10,20,300)	23.7	22.0	19.4	18.7
Bank/Canopy Distance (M) (0,10,50, 100)	18.9	22.0	24.4	24.4
Buffer Width (m) (0,15,30,50)	20.5	19.6	19.4	19.4

The most notable results from the cursory sensitivity analysis are that increasing the buffer width beyond 30 meters does not significantly decrease stream temperatures in this particular stream reach. Other vegetation parameters such as average tree height, and to a lesser extent bank/canopy distance, average canopy height and LAI have a stronger effect on stream temperatures.

The result that buffer widths beyond 30 meters do not significantly alter downstream stream temperatures arguably could be an artifact of a short reach length. To explore this possibility, a stream reach was chosen and the lengths were varied from 0.5 km to 15 km while all other parameters were held constant. The results are presented in Table 7.8.

Table 7.8: Simulated Stream Temperatures (°C) with Increasing Reach Lengths

Reach Length (km)	Buffer Widths (m)								
	0			15			30		
	avg	min	max	avg	min	max	avg	min	max
0.5	20.1	14.9	23.9	19.7	14.9	23.2	19.6	14.9	23.1
1	20.3	14.9	24.4	19.9	14.9	23.6	19.9	14.9	23.5
5	19.9	14.9	23.6	19.5	14.9	22.9	19.5	14.9	22.8
10	19.8	14.9	22.9	19.5	14.9	22.5	19.5	14.9	22.4
15	20.0	14.9	24.0	19.6	14.9	23.3	19.6	14.9	23.1
Maximum Difference	0.5	0.0	1.5	0.4	0.0	1.1	0.4	0.0	1.1

The results show that for stream reach lengths in the range of 0.5 to 15 km, the maximum stream temperature varies from 1.1 to 1.5 °C. The insignificant difference in predicted stream temperature with increasing reach length is most likely due to the upstream boundary condition used in this analysis. The minimum air temperature was used as the initial water temperature. This minimum air temperature is within 0.3 °C of the predicted stream temperature at the upstream boundary when a 3000 meter reach is modeled (see Section 6.2.2). This results needs to be studied in further detail to determine the appropriate reach length for use in the GIS-STRTEMP model. Currently, the model is limited by the requirement of a constant stream azimuth.

CHAPTER 8: CONCLUSIONS AND RECOMMENDATIONS

8.1 CONCLUSIONS

The GIS-STRTEMP stream temperature model, while based on physical principals, is easily implemented by planners, and accurately predicts maximum stream temperatures during the critical summer low flow period. The model incorporates the STRTEMP energy balance model (LaMarche et al., 1997) and is designed to replace empircial approaches like the Sullivan et al. (1990) algorithm currently incorporated in the Washington Forest Practices Manual. The model meets the two main objectives of this study. The first objective was to provide the basis for determining a potential maximum stream temperature based on 7Q10 low flow and 10 year maximum air temperature in forested mountain streams. The second objective was to provide a basis for determining the effects of differing vegetation parameters on potential maximum stream temperatures.

The GIS-STRTEMP model has five main components, shown graphically in Figure 8.1 and described in Chapter 4.
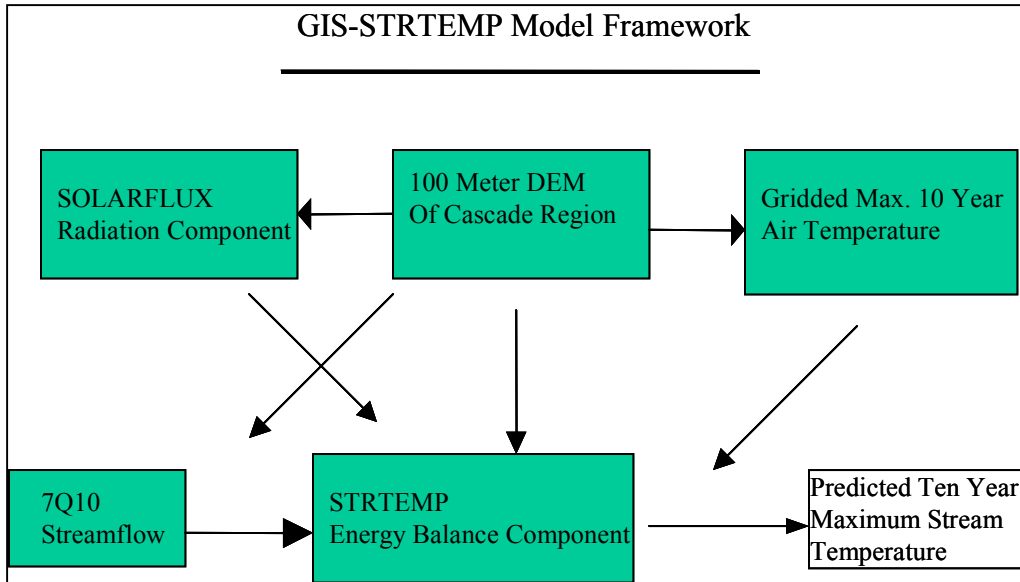
Figure 8.1: Graphical Representation of the GIS-STRTEMP model framework.

This study consisted of four parts; field data collection, 7Q10 low flow analysis, GIS-STRTEMP model development, GIS-STRTEMP model simulations, and sensitivity analysis. Field data was collected in the summer of 2000 in the Entiat and Beckler River basins to calibrate the model. The GIS-STRTEMP model is only valid in forested non-urban perennial streams in the Cascade Mountain Region with drainage areas less than about 1500 square kilometers. GIS-STRTEMP is a feasible tool for predicting maximum stream temperatures in the Cascade Mountain Region and is capable of predicting stream temperatures due to changes in the riparian vegetation. The GIS-STRTEMP model is only meant as a tool to determine stream reaches sensitive to certain stream temperature parameters and also to determine what a probable maximum temperature a stream is likely to experience.

The conclusions from the GIS-STRTEMP model study are as follows.

- Based on the sensitivity analysis and simulation results for this study, increasing the buffer width beyond 30 meters may not significantly decrease stream

temperatures in stream reaches like those studied in the Twisp and Suiattle River basins.

- Based on the sensitivity analysis and simulation results for this study average tree height, and to a lesser extent bank/canopy distance, average canopy height and LAI are significant parameters in determining stream temperatures.
- The upstream boundary condition does not significantly affect predicted stream temperatures if the condition is chosen appropriately.

8.2 RECOMMENDATIONS

This research has shown that the GIS-STRTEMP model can be a useful tool for planners in determining the following; the sensitivity of stream temperature to differing vegetation and physical parameters, the sensitivity of stream reaches with particular physical characteristics to changing physical parameters and particular stream reaches which may require more detailed field data and model analysis. Some recommendations for further research, based on the conclusions discussed in Section 8.1, are as follows.

- Evaluate in greater detail the effects of reach length and the upstream boundary condition on prediction of sensitivity of stream temperature to buffer width sensitivity.
- Evaluate in greater detail the importance of vegetation characteristics, such as, LAI, tree height and canopy height in determining stream temperatures.
- Modify the GIS-STRTEMP model to incorporate changing stream azimuths and vegetation parameters. This will allow for larger stream systems with changing riparian buffers to be evaluated.
- Obtain additional field data to evaluate the results from this study and also the parameters (such as 7Q10 low flow, LAI, air temperatures) estimated in the GIS-STRTEMP model.

LIST OF REFERENCES

Anderson, E.A. Development and testing of snowpack energy balance equations. Water Resources Research. Vol. 4. pp 19-37.

Beschta, R.L. and J. Weatherred. 1984. TEMP-84. A computer model for predicting stream temperatures resulting from the management of streamside vegetation. WDSDG-AD-00009. U.S.D.A. Watershed Systems Development Group. Ft. Collins, CO. July 1984.

Bowen, I.S. The ratio of heat losses by conduction and by evaporation from any water surface. Physical Review. Vol. 27. June, 1926. pp779-787.

Bristow, K.L. and Campbell, G.S., 1984. On the relationship between incoming solar radiation and daily maximum and minimum temperature. Agric. For. Meteorol., 31:159-166.

Brosofske, K.D., Chen, J., Naiman, R.J. and J.F. Franklin. 1997. Harvesting effects on microclimatic gradients from small streams to uplands in western Washington. Ecological Applications. 7(4): 1188-1200.

Brown, G.W. Predicting temperatures of small streams. Water Resources Research. Vol. 5(1). 1969. pp.68-75.

Brown, G.W. and Krygier, J.T. Effects of clear-cutting on stream temperature. Water Resources Research. Vol. 6. No. 4. August 1970. pp.1133-1139.

Buchmann, N., W.Y. Kao and J. Ehleringer. Influence of stand structure on carbon-13 of vegetation, soils and canopy air within deciduous and evergreen forests in Utah, United States. Oecologia, Berlin: Springer-Verlag. Vol. 110 (1). 1997. pp. 109-119.

Campbell, S.G. and J.M. Norman. An introduction to environmental biophysics. Springer-Verlag. 1998. 286 pp.

Chapra, S.C. Surface water-quality modeling. McGraw-Hill Series in Water Resources and Environmental Engineering. WCB/McGraw-Hill. 1997.

Daly, C., G. Taylor, and W. Gibson. The PRISM approach to mapping precipitation and temperature. 10th Conference on Applied Climatology. Reno,NV. American Meteorological Society. 1997. pp 10-12.

Dingman, S.L. Physical hydrology. Prentice-Hall, Inc. 1994. 575 pp.

Draper, N.R., and H. Smith. Applied regression analysis (2nd Ed.). Wiley, New York. 1981.

Helsel, D.R. and R.M. Hirsch. Statistical methods in water resources. Studies in Environmental Science 49. Elsevier Science Publishers. New York, NY. 1992

Hirsch, R.M., D.R. Helsel, T.A. Cohn, and E.J. Gilroy. Statistical Analysis of Hydrologic Data. Handbook of Hydrology. McGraw-Hill. 1993. pp. 17.1-17.55

Hynes, H.B.N. The ecology of running waters. University of Toronto Press, Toronto. 1970. 555 pp.

Jaske, R.T. Prediction of Columbia River Temperatures Downstream from Grand Coulee Dam for Wide Extremes of Flow and Weather Conditions. Pacific Northwest Laboratories, Battelle Memorial Institute, Richland, WA. September 1965. 19 pp.

LaMarche, J., T. Dubin and D.P. Lettenmaier. A 2-layer energy balance model for the prediction of stream temperature. American Geophysical Union Fall Meeting. 1997

Lee, R. and D.E. Samuel. Some thermal and biological effects of forest cutting in West Virginia. Journal of Environmental Quality. 1976. 5(4): 362-366.

Lynch, J.A., Corbett, E.S. and Hoopes, R. Implications of forest management practices on the aquatic environment. Fisheries. 1977. Vol. 2(2). pp.16-22.

Lynch, J.A., G.B. Rishel and E.S. Corbett. Thermal alteration of streams draining clearcut watersheds: Quantification and biological implications. Hydrobiologia. 1984. 111:161-169.

Monteith, J.L. and M. Unsworth. Principles of Environmental Physics. Edward Arnold. 1990. 291 pp.

O'Donnell, G., Bernt V. Matheussen, Alan Hamlet and Ed Maurer. Gridding NCDC daily meteorological data – Version 2. 1999. 13pp.

Penman, H.L.. Natural Evaporation from Open Water, Bare Soil and Grass. Proceedings of the Royal Society of London. Vol. A193. 1948. pp. 120-145.

Raphael, J.M. Prediction of temperature in rivers and reservoirs. Journal of the Power Division, Proceedings of the American Society of Civil Engineers. July 1962.

Rich, P.M., W.A. Hetrick, and S.C. Saving. Modeling topographic influences on solar radiation: A manual for the SOLARFLUX model. Los Alamos National Library. Manual LA-12989-M. 1994.

Rishel, G.B., J.A. Lynch, and E.S. Corbett. Seasonal stream temperature changes following harvesting. Journal of Environmental Quality. 1982. 11:112-116.

Salo, E.O. and Terrance W. Cundy. College of Forest Resources. Institute of Forest Resources. Streamside Management: Forestry and Fisheries Interactions. 1987. 467pp.

Sartoris, J.J. A mathematical model for predicting river temperatures-application to the Green River below Flaming Gorge Dam. Bureau of Reclamation. Denver, CO. Engineering and Research Center. Report REC-ERC-76-7. April 1976. 28 pp.

Selby, M.J. Hillslope material and processes. Oxford University Press. 1993. 451 pp.

Shepard, D.S. Computer mapping: the SYMAP interpolation algorithm. Spatial Statistics and Models. Reidel Publishing Company. Gaile and Willmott, eds. 1984. pp. 133-145.

Shuttleworth, W.J. Evaporation. Handbook of Hydrology. McGraw-Hill. 1993. pp. 4.1-4.53.

Sinokrot, B.A. and H.G. Stefan. Stream temperature dynamics: Measurement and Modeling. Water Resources Research. July 1993. Vol. 29. No. 7. pp 2299-2312.

Stedinger, J.R. and G.D. Tasker. 1985. Regional hydrologic analysis 1. Ordinary, weighted, and generalized least squares compared. Water Resources Research. 1985. Vol.21. No. 9. pp. 1421-1432.

Sullivan, K., J. Tooley, K. Doughty, J.E. Caldwell, P. Knudsen. Evaluation of prediction models and characterization of stream temperature regimes in Washington. Timber/Fish/Wildlife Rep. No. TFW-WQ3-90-006. Washington Department of Natural Resources, Olympia, Washington. 1990. 224 pp.

Tasker, G.D., and J.R. Stedinger. An operational GLS model for hydrologic regression. Journal of Hydrology. 1989. Vol. 111. pp. 361-375.

Theurer, F.D., K.A. Voos and W.J. Miller. Instream water temperature model. Instream Flow Info. Paper No. 16. U.S.D.I. Fish and Wildlife Service FWS/OBS-84/15. 1984

Thomas, S.C. and W.E. Winner. Leaf area index of an old-growth Douglas-fir forest estimated from direct structural measurements in the canopy. Canadian Journal of Forest Research. Vol. 30 (12). Dec 2000. pp 1922-1930.

Washington State Joint Natural Resources Cabinet. Statewide strategy to recover salmon – extinction is not an option. 1999.

USDA. Watershed assessment Entiat Analysis Area Version 2.0. Wenatchee National Forest. USDA, Forest Service, Pacific Northwest Region. April 1996.

Wissmar, R.C. and W.N. Beer. Distribution of fish and stream habitats and influences of watershed conditions, Beckler River, Washington. Fisheries Research Institute. FRI-UW-9418. October 1994.